ELECTRON SPIN RESONANCE STUDIES OF DEFECTS IN IONIC CRYSTALS

Thesis submitted to the University of Keele

for the Degree of Doctor of Philosophy

by

A.C. Tomlinson, B.A.

Department of Physics,
University of Keele,
Keele,
Staffordshire.

July, 1968.

ABSTRACT

Defects in single crystals of silver halides and calcium oxide have been investigated principally by electron spin resonance spectroscopy. Studies of the properties of iron dissolved in silver chloride and bromide have revealed that threshold temperatures exist below which Fe^{2+} cannot trap a hole during illumination. In the case of silver chloride, a trigonal Fe^{3+} spectrum is formed after irradiation at about 170°K. Warming the crystal to 200°K converts this spectrum to a cubic spectrum, which is interpreted as arising from the migration of an Ag^{+} ion away from the complex. In silver bromide no trigonal spectrum from Fe^{3+} has been detected. Instead illumination at about 160°K produces the cubic Fe^{3+} spectrum, at characteristically lower temperatures than that for the equivalent complex in silver chloride. Attempts to observe the ions V^{2+} and Mn^{4+} in silver chloride, and Cu^{2+} in silver bromide have been unsuccessful.

The use of relatively unstrained crystals of calcium oxide has made possible resolution of the hyperfine structure of the isotopes 155 and 157 of gadolinium in cubic symmetry, and also the transferred hyperfine structure of the (single electron) F^{+} centre from ligand Ca^{43} (0.13% abundant) and O^{17} (0.037% abundant). Investigation of electron and hole trapping processes during ultraviolet irradiation has revealed a new spectrum in chemically reduced crystals, which has been attributed

to Ti^{+} ions on substitutional octahedral sites. Oxidizing annealing and quenching studies indicate that hole centres may be created by heat treatment alone, and a new centre containing two holes, not previously observed in calcium oxide is reported. The strain induced by quenching enables double quantum transitions in the Mn^{2+} spectrum to be observed.

ACKNOWLEDGMENTS

The author would like to thank:

Professor D.J.E. Ingram for his continued encouragement, supervision of this work and the use of laboratory facilities.

Dr. B. Henderson for valuable discussions and the loan of the Varian spectrometer and the calcium oxide crystals.

All members of the department for co-operation and assistance.

Miss K. Davies for her care and patience in typing this thesis.

CONTENTS

CHAPTER I

INTRODUCTION

Electron Spin Resonance (E.S.R.) is a spectroscopic method for detecting transitions between spin states of unpaired electrons in a magnetic field. The crystals considered in this thesis are not paramagnetic in their pure undamaged state. However many defects which may be introduced are paramagnetic and hence one may use E.S.R. as a technique for studying them. In fact E.S.R. and ENDOR (Electron Nuclear Double Resonance) are the only means of what one may call an "atomic scale microscopy" which enable a detailed picture or model of the defects and their energy level systems to be obtained.

The variety of defects that can occur in ionic crystals is extensive and the present interest centres upon what may loosely be termed point defects, implying that the defect centre is localized. This is in contrast to such systems as dislocation lines which are essentially extended over several lattice spaces. Point defects may be subdivided into intrinsic and extrinsic defects. An intrinsic defect occurs when a localised disorder exists solely among the ions native to the lattice. A simple example is a missing ion: a vacancy. Indeed it can be shown on thermodynamic grounds that in an otherwise perfect crystal some vacancies must exist at finite temperatures. At high temperatures, near the melting point, the numbers of such defects may be in excess of any other defects. In the silver halides, silver ions

leave their lattice sites and remain in interstitial sites. Such defects are known as Frenkel defects. On the other hand in the alkali halides and the alkaline earth oxides, ions leave their lattice sites and migrate to boundaries of the crystal. This type of disorder is known as Schottky disorder, and in predominantly ionic lattices there must be roughly equal numbers of anion and cation vacancies left to maintain local charge neutrality. By themselves neither interstitial ions (of these crystals) nor vacancies are paramagnetic and are thus of no interest to the E.S.R. spectroscopist. However their existence and possible interaction with defects that are paramagnetic is of considerable importance.

Extrinsic point defects occur when "foreign" atoms or ions are found in crystals. Even in the purest materials available there are probably in excess of 10^8 impurity atoms per cubic centimetre, and in most crystals at ordinary temperatures the impurity defects will far outnumber the natural defects mentioned above. This has important implications because impurities unintentionally incorporated in crystals may give rise to effects which are attributed to other defects, or even basic properties of the material.

In Chapter II intrinsic and extrinsic defects are discussed in more detail. Chapters III and IV are devoted to the theoretical and practical aspects of E.S.R. spectroscopy. Chapter V discusses some of the handling techniques used for the crystal materials, and Chapters VI and VII report the results obtained from E.S.R. studies of defects in silver halide and calcium oxide single crystals. ChapterVIII concludes by summarising the results obtained.

CHAPTER II

INTRINSIC AND EXTRINSIC DEFECTS IN IONIC CRYSTALS

2.1 Intrinsic Defects

As previously mentioned vacancies, and in some cases interstitial ions, will occur in otherwise pure and perfect crystals. These vacancies cannot be observed either by E.S.R. or optical spectroscopy unless they have either an excess or deficit of electrons. This is because there will be no electronic energy levels between which transitions may be induced. An anion vacancy, however, can trap one or more electrons, because it is essentially a missing negative charge, and will thus attract any negative entity which is sufficiently near for the coulombic forces to dominate the purely random thermal motion. Electrons in the conduction band of an ionic crystal are highly mobile in the lattice, and when they approach an anion vacancy it is energetically favourable for them to be trapped. The de Boer model of an F centre is precisely an electron trapped at an anion vacancy, and is shown in Figure 2.1a. The following definitions of F centres will be adhered to in this thesis to keep in line with a review of defect centres in the oxides (1). A simple F centre is a single anion vacancy which has trapped electrons to become charge neutral. In the alkali halides this means an F centre is a one electron centre, but in the alkaline earth oxides it is a two electron centre. Other electrons containing centres will be denoted by charge superscripts, for example a single electron trapped at an anion vacancy

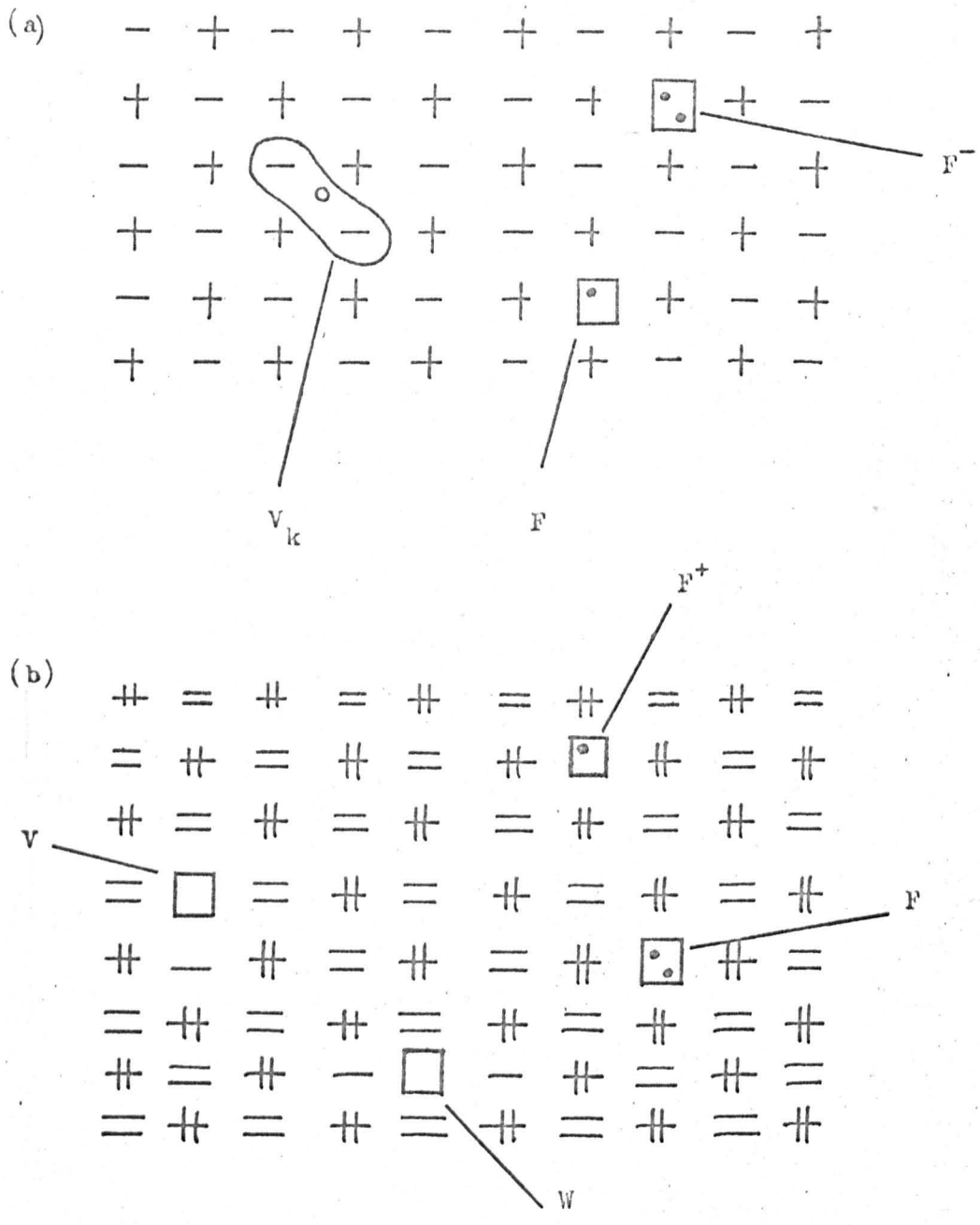

Figure 2.1. Intrinsic defects in ionic crystals.
(a) monovalent lattice, e.g. NaCl.
(b) divalent lattice, e.g. CaO.
Note the essential difference between the types of V centre found in the different lattices.

□ vacancy • electron ○ hole

in calcium oxide will be called the F^+ centre because it introduces a local positive charge into the lattice. These are illustrated in Figure 2.1.

By far the greatest amount of work on F centres has been carried out in the alkali halides. The name itself derives from the German work "farben" meaning colour, because in the nineteen twenties it was found that crystals of alkali halides could be coloured by certain techniques. Within fairly large experimental errors it was found that the absorption bands produced in the visible region of the spectrum were independent of their means of production. These methods included electron injection from a pointed electrode at high temperatures, X-raying at lower temperatures, and heat treatment in metal vapour followed by quenching. While many of the experiments strongly suggested that the centre causing the absorption band was an electron centre perhaps associated with anion deficient lattices, it was not until E.S.R. techniques became available that the de Boer model was verified for the F centre in the alkali halides.

E.S.R. of F centres in alkali halides revealed g values less than the free spin value 2.0023 and it was shown (2) that there must therefore be an appreciable orbital contribution of the magnetic moment of the F centre electron. This was assumed to come from the ions surrounding the vacancy. The nearly Gaussian shape of the resonance line, and its relatively large breadth was accounted for by interaction of the electron with the nearest and next-nearest neighbour shells of ionic

nuclei principally via the S orbitals of the ions (3). In the alkali halides there are large proportions of the ions which have non zero nuclear magnetic moments and therefore in most cases resolution of the spectrum into discrete components is impossible. However the use of the ENDOR technique by Feher (4) rendered this unnecessary as it was possible to assign the resonances to particular ions and determine the angular variations of the spectrum. In some cases the overlap of the electron on its neighbours has been measured out to the eighth shell by the ENDOR method. In the alkali halides it has been this experimental method that has positively verified the de Boer model, as none of the alternatives predicted the right symmetry and were sufficiently stable.

The optical absorption band first studied as an aspect of the F centre has been correlated with the E.S.R. spectra with a fair degree of certainty by bleaching experiments in which both spectra diminished by the same amount. A second, broader optical band was formed which was called the F' band, and has been assigned to two electrons trapped at one anion vacancy. Thus on the previous definitions it will be called the F^- band or F^- centre. The single vacancy has the power to trap a second electron because the F centre electron is spread over such a large amount of lattice, there is a net positive charge remaining in the locality of the vacancy. The F^- centre has two electrons which are paired off and hence no E.S.R. may be observed from it, and there are apparently no excited states within the band gap so no triplet states exist for this centre. The broad optical absorption band attributed

to the F^- centre is thought to arise from a ground state to conduction band transitions. In the alkali halides this centre is not stable at room temperature because of the small ionization energy of the second electron. Since no E.S.R. has been observed from this centre, positive models do not exist, but careful cross bleaching experiments reveal that the destruction of one F^- centre results in two F centres, which strongly implies that it is a two electron centre.

F centres have not been observed in the silver halides, probably because Frenkel disorder predominates and only cation vacancies are formed in appreciable numbers, but they have been observed in the alkaline earth oxides. A reasonable correlation has been established between optical and E.S.R. spectra. Among these oxides most attention has been paid to magnesium oxide, and the de Boer model for the F^+ centre verified from E.S.R. alone (5), which is shown in Fig. 2.1b. This has been possible because 90% of Magnesium has no nuclear spin and 10% is Mg^{25} with $I = 5/2$. It is thus probable that the F^+ centre will have none, one or two Mg^{25} ions as nearest neighbours, and spectra from these three cases have been resolved. The case of calcium oxide is extremely unfavourable for observation of nuclear magnetic interactions with the F^+ centre as the only natural isotopes with nuclear moments are the 0.13% abundant Ca^{43} and the 0.037% abundant O^{17}. An isotropic resonance with $g = 2.0000$ and an optical absorption at 3.65eV have been attributed to the F^+ centre from Faraday rotation studies (6). Some work on powders of calcium oxide artificially

enriched with Ca^{43} and irradiated to produce F^+ centres has revealed the principal hyperfine parameters for the interaction with the nearest neighbours, but only by assuming the de Boer model (7). Work reported in this thesis on single crystals of calcium oxide with the naturally occurring concentrations of Ca^{43} identifies the resonance at 2.0000 as arising from the de Boer F^+ centre. Furthermore the interaction with the second shell of neighbours has been observed, from the naturally occurring O^{17}. In both these cases the possibility of more than one magnetic nucleus being a nearest or next-nearest neighbour is so small it may be neglected.

An optical absorption band occurring in additively coloured calcium oxide at 3.1eV has been assigned to the F centre (2 electrons, Figure 2.1b). Some support for this has come from cross-bleaching experiments in which light excitation in this band enhanced the F^+ E.S.R. spectrum (8). The implication is that from an excited state of the F centre an electron may be thermally excited into the conduction band and diffuse away leaving an F^+ centre. These qualitative experiments have been repeated, but in addition a long lived red fluorescence was observed after irradiation into the 3.1eV band. It was thought possible that this might arise from a triplet to singlet transition of the F centre because of its long lifetime. Since a triplet state is paramagnetic, a resonance was sought which was present only during or immediately following light excitation. Such a resonance was indeed found, which was initially assigned to a triplet state of the

F centre. Further investigation of the transient behaviour of this spectrum revealed that it did not arise from an excited state, but rather a ground state, and the hyperfine structure associated with it showed that it was due to an extrinsic defect, since it was isotropic. The spectrum has finally been assigned to substitutional Ti^+ ions.

Only heavy particle irradiation will produce anion vacancies in the alkaline earth oxides. X-rays and γ-rays cannot transfer sufficient momentum to an anion to cause displacement. F^+ and F centres have been produced by additive colouration, which involves heating the crystals in metal vapour. Evidently a general chemical reduction takes place under such circumstances (9), and impurity cations may be reduced in valency. Analogously the reverse action may be obtained by annealing in oxygen, which produces cation vacancies. These are not normally populated by holes although a small proportion may be as is reported later in this thesis. The proportions of hole containing cation vacancies may be enhanced considerably by ionizing radiation, more efficiently in calcium oxide than in magnesium oxide. During irradiation electron-hole pairs are formed. This means in the case of ionic solids that electrons are ejected from anions leaving them effectively positively charged. Neglecting the possibility of immediate recombination, the electron wanders away and is trapped elsewhere. The electron deficiency or hole hops from anion to anion until it is trapped at a cation vacancy which has a net double negative charge. E.S.R. results suggest that the simple cation vacancy may trap one or two holes both in MgO (10)

and in CaO (this thesis). In either case the centre is axially symmetric at low temperatures with the hole trapped on one anion for the first case, called a V centre, and two holes trapped on anions on opposite sides of the cation vacancy in the second case, called a W centre, as shown in Figure 2.1b. At higher temperatures the holes hop rapidly from one anion to the next, resulting in an extremely broad spectrum. There is no evidence to suggest that the molecular complexes formed in the alkali halides by additive colouration have analogues in the alkaline earth oxides. An example of such a centre is the V_K centre, shown in Figure 2.1a.

In this section only the simplest of the possible intrinsic defects of interest to E.S.R. spectroscopists have been discussed. Many more complex centres exist and have been extensively studied.

2.2 Extrinsic Defects

Extrinsic defects occur where an impurity ion, atom or molecule is present in the lattice. As with intrinsic defects E.S.R. and optical measurements compliment one another but care must be taken to ensure that there is a one to one correspondence for the spectra. This is generally fairly easy in the silver halides where highly pure materials are available through zone refining techniques. In such cases the quantity of impurity deliberately introduced may dominate by several orders of magnitude the other accidental impurities. This considerably eases the problems of interpretation. In the case of the alkaline earth oxides zone refining is not possible and furthermore the methods

available for single crystal preparation involve using large amounts of starting materials, effectively precluding the use of very high purity materials on economic grounds. In any case impurities are most likely introduced in the growth stage. In consequence deliberately introduced impurities are often at best only an order of magnitude more concentrated than other impurities, and optical spectra are more difficult to assign with certainty. Many defects are known by their E.S.R. spectra alone. This does have the advantage however that interesting results may be found for accidental impurities, well exemplified in the present work which reports observations on titanium and gadolinium ions, neither of which had been deliberately introduced. In addition, in the crystals of calcium oxide many other impurities were detected by E.S.R. and provided a useful guide to the state of the crystal.

E.S.R. provides an extremely powerful technique for identifying paramagnetic impurities. The valence state and the symmetry of the local environment can generally be determined unambiguously. For impurities to be paramagnetic it is necessary for them to have unpaired spins. Impurity ions with unpaired spins most frequently come from one of the transition metal series. The first of these occurs when the 3p shell is filled, and further electrons go into the 3d or 4s shells. In the crystal the metal is generally ionized and one can simply consider the 3d electrons as a first approximation. Provided these paramagnetic ions are sufficiently far apart to neglect possible exchange interactions between them, which is generally satisfied for dopings of 1000 parts per

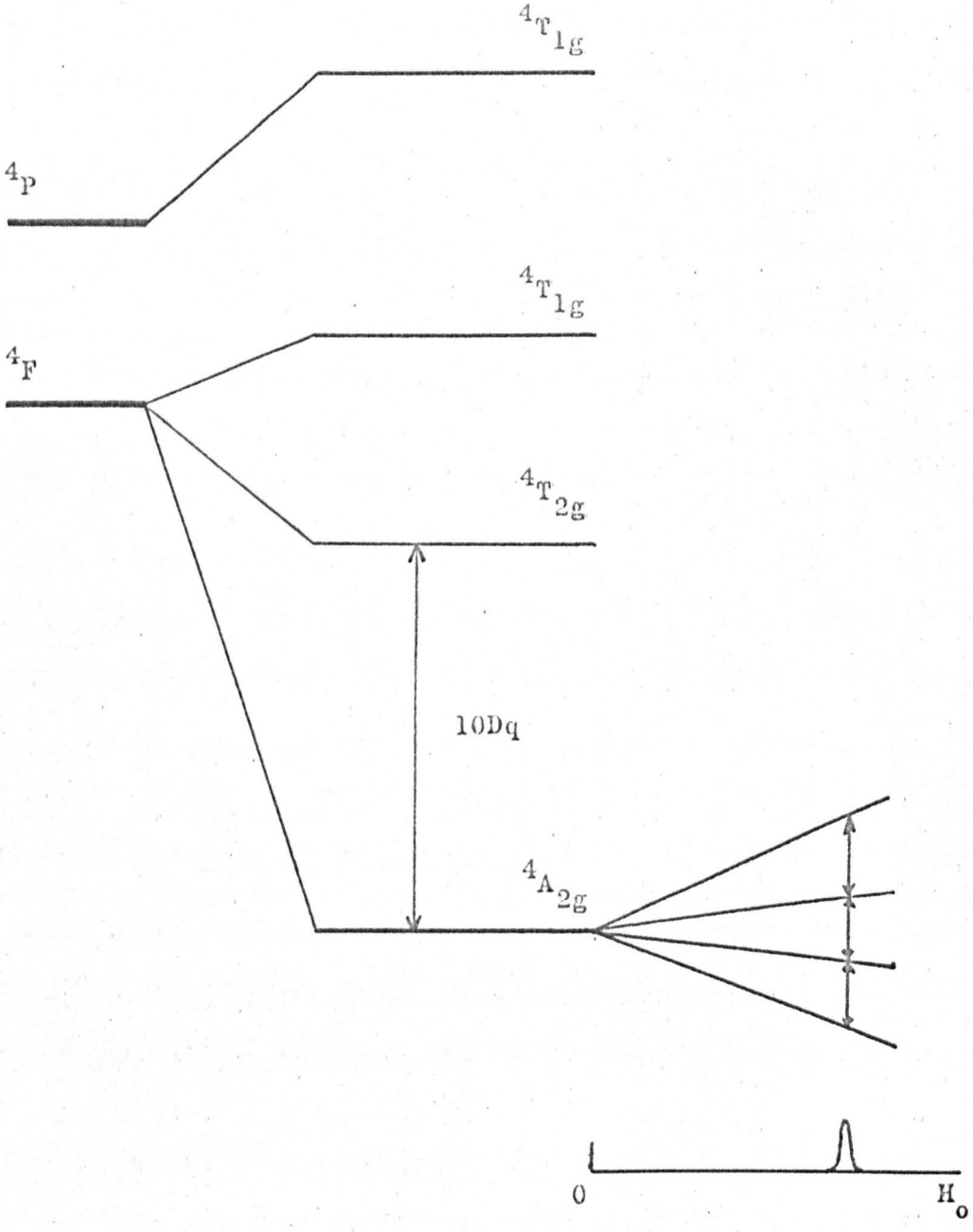

Figure 2.2. Energy levels of $3d^3$ ions in octahedral crystal field. Zeeman splitting of ground level shown for case when the nuclear spin I=0.

million (ppm) or less, quantum theory may be applied to them as if they were isolated ions acted on by the electric field of appropriate symmetry and strength from the neighbouring closed shell ions.

In order to make the ideas more concrete, a specific example will be chosen. Consider the case of a $3d^3$ ion in the calcium oxide lattice. Any of the ions Ti^+, V^{2+}, Cr^{3+} or Mn^{4+} would be a $3d^3$ ion and most of these have been previously reported in calcium oxide (11). One cannot judge a priori what site the ions would take, i.e. substitutional or interstitial, nor what the symmetry would be, i.e. whether there was localised charge compensation. In fact it is believed that each of these ions most commonly occupies a substitutional site with octahedral symmetry implying that charge compensation when necessary is remote from the ion. Thus in this case the ion will be subjected to the electric field of six O^{2-} ions which will have octahedral symmetry. A $3d^3$ ion has 21 electrons, 18 of which fully occupy the orbitals of the configurations $1s^2$, $2s^2$, $2p^6$, $3s^2$, $3p^6$ which constitutes the argon closed shell configuration. The remaining 3 electrons occupy 3 out of the 10 available 3d orbitals. The argon shell may now be neglected and only the $3d^3$ electrons need to be considered. Applying Hund's rule it is found that the lowest level is the quartet ^4F. This implies that $L = 3$ and $S = 3/2$. Group theoretical considerations show that in a purely cubic field the sevenfold orbital degeneracy will be split into a singlet and two triplets lying higher in energy as shown in Figure 2.2. The four fold spin degeneracy of the lower singlet will not be lifted and the

E.S.R. spectrum will consist of a single isotropic line in the absence of other interactions such as, for example, nuclear hyperfine interactions. Owing to the relatively large crystal field splitting, of about $10^4 cm^{-1}$, the orbital moment is largely quenched and the g value will be near but less than the free spin value. In fact each of the ions mentioned has naturally occurring isotopes with non zero nuclear spins and hence the single line is split. This makes identification of the different $3d^3$ ions relatively simple. In the case of vanadium for example, the 100% abundant ^{51}V has nuclear spin I = $^7/_2$ and thus there is an eightfold splitting of the line, neglecting the possibility of forbidden nuclear and electron transitions. Second order perturbation theory shows that as a result of the nuclear splittings the degeneracy of the fourfold spin is partially removed (12). This results in a small angle dependent splitting of each of the eight lines into three components. The two outer components, being the $\Delta M_s = \pm\frac{1}{2} \rightarrow \pm\ ^3/_2$ transitions are frequently broadened by the presence of small axial distortions arising from nearby crystal imperfections as a result of the sensitivity of the energy separation $\pm\frac{1}{2}$ and $\pm^3/_2$ levels via spin orbit coupling from splitting of the excited state orbital triplet by axial fields. In cases where spectra are weak they may be broadened beyond detection. The $\frac{1}{2} - \frac{1}{2}$ transition is unaffected by these considerations and remains completely isotropic. The spectrum is easily observable at room temperature, because spin lattice relaxation is not too fast, although some broadening is evident.

In cases where the paramagnetic impurity is unknown the nuclear splitting of the ion itself can provide valuable assistance in identification, as most of the iron transition group has at least one isotope with non-zero nuclear spin. The charge or degree of ionization can generally be determined from the characteristics of the E.S.R. spectrum, for example in the case of vanadium previously mentioned, the trivalent form V^{3+} is a ^3F state. The crystal field splitting leaves an orbital triplet lowest, which is unstable according to the Jahn-Teller theorem (13). This results in a spontaneous distortion leaving an orbital singlet lowest. Spin orbit coupling introduces a further splitting leaving the $M_s = 0$ level below the $M_s = \pm 1$ level. The close energetic proximity of these levels implies a fast spin lattice relaxation time and low temperatures are generally required for observation of E.S.R. If the zero field splitting between the $M_s = 0$ and ± 1 levels is larger than the microwave quantum used for Zeeman measurements, no resonance will be observed, except possibly the $\Delta M_s = 2$ forbidden transitions. These considerations in conjunction with information about the chemical state of the crystal enable an unambiguous interpretation of this spectrum as arising from V^{2+}. In fact no resonance has been observed down to $1.3^{\circ}K$ which has been attributed to a $3d^2$ ion in the alkaline earth oxides (1).

Another possibility is that ions may be interstitial, in which case the coordination of the ligand ions is tetrahedral or eightfold cubic. In the case of $3d^3$ ions this crystal field reverses the orbital levels and a triply degenerate level lies lowest. This would result

in a distinct E.S.R. spectrum because again the Jahn-Teller effect would result in distortions of the complex producing anisotropic resonances which are not in fact found.

The above possibility may be considered fairly remote on other grounds however, particularly the ionic size of V^{2+} and the amount of space in the calcium oxide lattice. In the framework of ideas embodied in the quantum theory, according to which the electron wave function has a spatial distribution about its nucleus described by exponentials, the concept of a definite ionic radius for a particular ion may seem somewhat unrealistic. However there is considerable evidence that the ionic radius for a particular ion does not vary by more than a few percent over a wide range of environments. It can easily be seen that it is extremely unfavourable energetically for an ion to go interstitially into the calcium oxide lattice. The large bonding energy of the lattice, shown for example by the high melting temperature would strongly resist the lattice distortion necessary, Rare earth ions, because of their large radius, will not enter the magnesium oxide lattice even substitutionally with ease. In the silver halides, on the other hand, Fe^{3+} is known to occupy a substitutional site for preference (14), and this is probably the result of several factors. Firstly it forms a strongly bound complex with four ligand halogens, which is only possible in the interstitial site without upsetting the crystal structure considerably. Secondly it has a large excess charge and would require two silver ion vacancies for charge compensation, which is generally local in the case of the silver

halides. This is because the Ag^{+} ion has a low activation energy for interstitial migration, in contrast to the alkaline earth oxides with a higher activation energy, and generally remote charge compensation.

Referring to the zero field energy levels in Figure 2.2, it can be seen that it would be possible in principle to obtain optical absorption transitions between the various energy levels of the ion in the crystal field. For the case of Cr^{3+} in MgO this has indeed been reported (15), and provides an excellent example of optical and E.S.R. data complementing one another in the detailed investigation of a defect. It is worth restating, however, that in such crystals the assignment of optical absorption spectra due to extrinsic defects is a difficult task, with many uncertainties. In the present instance a band at 16,200cm^{-1} could not with certainty be assigned to a transition, but no other impurities were considered as being candidates for the production of this band, yet it is certain many other impurities were present in considerable concentrations.

CHAPTER III

ELECTRON SPIN RESONANCE PRINCIPLES AND INTERPRETATIONS

3.1 The Resonance Conditions

The possession of both angular momentum and charge confers on an electron a magnetic moment $\underline{\mu}$ which is proportional to the angular momentum $\underline{J}$

$$\underline{\mu} = -\gamma \underline{J} \qquad 3.1$$

where the proportionality constant γ is called the gyromagnetic ratio. The angular momentum $\underline{J}$ will generally be a combination of spin and orbital angular momentum, but as will be seen, in many cases for paramagnetic ions situated in a crystal electric field, the orbital contribution to J is largely quenched and 3.1 may be replaced by:

$$\underline{\mu} = -g\beta \underline{S} \qquad 3.2$$

where g is the spectroscopic splitting factor for the electron, β is the Bohr Magneton equal to $e\hbar/2mc$ where -e is the charge and m the mass of the electron, and S is the spin angular momentum of the electron. For a single free electron $S = \frac{1}{2}$ and $g = 2.0023$, but in paramagnetic resonance experiments one may be concerned with more than one electron in each system, hence S may be greater than one half and departures from the free spin g value are common, due to some admixture of orbital angular momentum via the spin orbit interaction.

The interaction between the electron spin and the magnetic field may be represented by a simple spin Hamiltonian H_s,

$$H_s = \beta \underline{H} . \underline{\underline{g}} . \underline{S} \qquad 3.3$$

where $\underline{H}$ and $\underline{S}$ are vector quantities and $\underline{\underline{g}}$ is a tensor. For a single electron with $S = \frac{1}{2}$ there are two allowed orientations of the electron in the field H_z. Application of a radio frequency oscillating magnetic field H_1 perpendicular to H_z induces magnetic dipole transitions between the two allowed orientations provided the resonance condition:

$$h\nu = g\beta H \qquad 3.4$$

is met. The energy $h\nu$ of the quanta of the radio frequency photons is just the difference in energy of the two spin states ($M_s = \frac{1}{2}$) - ($M_s = -\frac{1}{2}$) in the magnetic field and the transition is allowed as the condition for magnetic dipole transitions is $\Delta M_s = 1$.

Typical frequencies for ν are 9.4kMc/s (X-band) and 35kMc/s (Q-band), which require magnetic fields of 3,400 and 12,500 gauss respectively for spin resonance of the free electron. These frequencies are convenient because the Zeeman energy is then greater than the other interactions with the electron spin for many situations making the interpretation of spectra much simpler. For most experimental situations the sensitivity increases with frequency which means using higher frequencies is an advantage where weak signals are being investigated.

Where broadening of an E.S.R. line is occurring because of g value variations, the linewidth will be proportional to frequency, and using a higher frequency may resolve broad lines into discrete components. In general where broadening is due to hyperfine interactions, or random axial crystal fields with energies small compared with the Zeeman energy, the linewidth will be independent of the microwave frequency. Interpretation of spectra may be facilitated by measurements at more than one frequency in some cases.

3.2 Paramagnetic Defects subjected to Crystal Fields

For the case of impurity ions with unfilled shells subjected to the electric field of the diamagnetic ions of the crystal, the energy levels split up in a rather different way from the same free ion. Three cases may usefully be distinguished for the effect of the crystal field on the ion. The weak field case is exemplified by the rare earth ions. The magnetic electrons belong to the 4f shell, which lies well within the core of the ion and so do not interact strongly with the crystal field. Thus the crystal field interaction is weaker than both the Russell Saunders coupling (s.s and $\ell.\ell$) and the spin orbit coupling (ℓ.s) between the 4f electrons. The total L and S are coupled to give states characterised by the total angular momentum J which has degeneracy (2J + 1), and consequently g values vary widely from the free spin value. Exceptions are the $^8S_{7/2}$ ions Gd^{3+} and Eu^{2+} which have half filled shells and consequently no contribution in first order from the orbital momentum.

The medium field case includes many of the iron group ions with unfilled 3d shell. These electrons are strongly exposed to the crystal field, which may be represented in the simplest approximation as negative point charges in the case of ionic crystals. The crystal field dominates the spin orbit coupling and the way the fivefold orbital degeneracy $(2\ell + 1)$ is split by the crystal field depends on the symmetry of the ligand ions. Individual cases will be considered as they arise in the presentation of the results. However considering a d^3 system subjected to an octahedral field, group theoretical considerations show (16) that a singlet orbital state lies lowest with $S = {}^3/_2$ which is unsplit by the octahedral field. Hund's rule requires that $S = {}^3/_2$. The next levels lie about $10{,}000 cm^{-1}$ above this triplet and this splitting is known as the crystal field splitting Δ. This parameter may be determined in some cases by optical spectroscopy (e.g. 15). Departures from cubic symmetry introduce a small splitting between the $\pm{}^3/_2$ level and the $\pm{}^1/_2$ level.

The so called strong field case occurs when the crystal field splitting is larger than the Russell-Saunders coupling energy. This means that it is energetically unfavourable for electrons to give maximum S (Hund's rule) rather than pair off in the lower orbital levels. An example is afforded by Fe^{3+} (d^5) in certain complexes. Assuming octahedral symmetry, the orbital levels are split as for d^3 complexes into a lower triplet and an upper doublet. For medium crystal fields the electrons occupy all the orbital levels and the Pauli

principle allows Hund's rule to be satisfied and S = $5/2$. In a strong crystal field, however, the electrons pair off in the lower orbitals leaving S = $\frac{1}{2}$. Examples are given by the complexes $\{Fe^{3+}(O^{-})_6\}^{3-}$ which is medium field, and $\{Fe^{3+}(CN)_6\}^{3-}$ which is strong field or low spin. Most of the 4d and 5d complexes are strong field cases.

At this point it is worth stating the results of two theorems which have important implications for the interpretation of E.S.R. spectra. Firstly Kramers Theorem states that a level with half integral J, cannot have all its degeneracy removed by an electric field alone. At most an electric field will leave a level split into a series of doublets. The doublets may split under the influence of a magnetic field. This implies that a system containing an odd number of electrons cannot have a singlet (orbit and spin) level as a ground state, and resonance is always in principle possible (13). Secondly the Jahn-Teller theorem indicates that for a system with an orbitally degenerate ground state, distortion will spontaneously occur to remove as much degeneracy as possible. Thus it follows that the orbital plus spin degeneracy of the ground state of a complex will be a singlet if it contains an even number of electrons, and a maximum of (2S + 1) if it contains an odd number of electrons (13).

3.3 The Spin Hamiltonian

The E.S.R. spectrum may be summarised by the Spin Hamiltonian, which provides an extremely compact and convenient way of representing what may be a spectrum consisting of a large number of lines with complex

angular dependence on magnetic field orientation. This method of presentation of results was first derived by Abragam and Pryce (17) and may be represented by:

$$H_s = \beta \underline{S}.\underset{\sim}{g}.\underline{H} + D\{S_z^2 - S/3(S+1)\} + E(S_x^2 - S_y^2) + \frac{a}{6}\{S_x^4 + S_y^4 + S_z^4 - \frac{1}{5}S(S+1)(3S^2+3S-1)\}$$

$$\underline{S}.\underset{\sim}{A}.\underline{I} + \sum_n (\underline{S}.\underset{\sim}{A}_n.\underline{I}_n - \mu \underline{I}_n.\underset{\sim}{g}_n.\underline{H}) \qquad 3.5$$

The above is a fairly general Spin Hamiltonian but does not include all possible interactions, for example certain electric field symmetries would require extra terms. No mention has been made of nuclear quadrupole interactions which always exist when $I > \frac{1}{2}$, but these are generally very small, and appropriate terms may be included to cover such cases when the effect is appreciable. The first term in 3.5 is the electron Zeeman term, which governs the interaction of the electrons with the applied magnetic field $\underline{H}$. At the microwave frequencies mentioned above this is the dominant term for most experimental situations. Since $\underline{S}$ and $\underline{H}$ are both vector quantities g is a tensor, which may usually be diagonalized along suitable crystal axes. It is a measure of the spin and orbital contributions to the paramagnetism, and in different experimental situations varies from about 0.1 to 18. It is analogous to the Landé splitting factor g_J for free ions but generally is different for ions in crystals. In particular many of the first transition metal complexes have their orbital momentum effectively quenched and deviations from the free electron g value are small and come from spin orbit coupling to excited states. Many intrinsic defect centres also have g values

near 2. The parameter $\underline{S}$ is a spin operator representing either the true spin or in some cases a fictitious spin for a low lying state separated by a zero field term from other electronic levels. The magnetic dipole moment associated with spin S has 2S + 1 allowed orientations with respect to the field H, with corresponding magnetic quantum numbers $M = S, S-1 \ldots -S$ and relative energies $g\beta HM_s$. In the resonance experiment there are 2S allowed transitions with $\Delta M_s = \pm 1$ between these levels which occur at the same field in the absence of other interactions. For example the $3d^3$ ion Cr^{3+} has $S = 3/2$ and in cubic fields the three transitions occur at precisely the same field for the even nuclear isotopes with I = 0. When $I \neq 0$ however small differences in field occur even for the transitions occurring from the same nuclear level. The g value may always be reduced to three values g_x, g_y, g_z, which means the first term in 3.5 may be rewritten $(g_x H_x S_x + g_y H_y S_y + g_z H_z S_z)$, reducing to $\beta g_z H_z S_z$ when H is in the z direction.

The three remaining terms in the first line of 3.5 are electron Stark terms arising from the electric field symmetry of the centre, and give rise to splittings of the orbital ground term when $S > \frac{1}{2}$. The first of these occurs when a single axial distortion of the cubic field is present, and the second when the symmetry is lower than axial. The third term always occurs in cubic symmetry or lower for $3d^5$ ions with $S = 5/2$, and analogous terms occur for $4f^7$ ions with $S = 7/2$. While the full reasons for the occurrence of these terms is not always known, the behaviour of the spectrum under magnetic field rotation, and hence the

value of these parameters can give valuable information concerning the value of S and the detailed symmetry of the centre. Typical values of D, E and a are between a few gauss and many thousands of gauss in some cases of D.

The terms in the second line of 3.5 arise from nuclear interactions. The first of these is the interaction of the unpaired electrons with their own nucleus. Thus it is always zero for F centres which have no nucleus, being centred on a vacancy. The interaction is frequently isotropic and hence the term may be rewritten $A\underline{I}.\underline{S}$, where A is a scalar quantity. The magnitude of A is usually between a few gauss and a few tens of gauss, and since the electron wavefunction for d electrons is essentially zero at the nucleus, the explanation of the existence of non-zero A terms must involve s electron wave functions. It is generally assumed that configuration interaction mixes small amounts of 3s and 4s character into the magnetic electron wavefunction. The isotropic hyperfine interaction is an extremely valuable parameter for identifying unknown ions. Since the selection rules operative in an E.S.R. experiment are $\Delta M_S = \pm 1$, $\Delta M_I = 0$ and the nucleus can take up $2I + 1$ orientations in the magnetic field, the value of I can be determined by counting the $2I + 1$ lines. Some transition metal ions have more than one nucleus with non zero nuclear magnetic moment in which case identification may be doubly checked.

The last terms are the transferred hyperfine interaction and the nuclear Zeeman interaction summed over the neighbours of the para-

magnetic centre. In electron spin resonance by itself it is usually sufficient to consider the nearest or, at most, nearest and next nearest shells of ions as contributing to the spectral broadening or splitting of the transition. The tensor $\underset{\sim}{A}_n$ can again be diagonalized into three axes but these are not necessarily the axes of the g value. In cubic crystals this is usually the case however and the whole term $\underline{S}.\underset{\sim}{A}_n.I_n$ may be divided into two parts; the isotropic interaction $a_n I_n.\underline{S}$ and the anisotropic interaction $B_x I_x.S_x + B_y Y_y.S_y + B_z I_z.S_z$. The isotropic part may give information about the electron wavefunction density at the nucleus concerned, and hence a detailed picture of the extent of delocalization of the centre built up. The anisotropic part is particularly useful for determining the exact symmetry of the site, for example the de Boer model of the F centre has been confirmed by this interaction in many materials. It is most powerful as it enables a definite conclusion to be reached on the type of cubic symmetry present, i.e. eight, six or fourfold coordination, which electron Stark terms alone, even if present, cannot do.

3.4 Energy Levels in a Magnetic Field

The experimentalist's problem is to determine the parameters in the Hamiltonian from the recorded spectrum. The spin Hamiltonian H_s is related to the energy levels of the system by the Schroedinger equation

$$H_s \psi = E \psi \qquad 3.6$$

where ψ is the wave function of the magnetic electrons. The eigenvalue E must satisfy 3.6, so it becomes:

$$(H_s - E)\,\psi = 0 \qquad 3.7$$

and hence the eigenvalues are given by the roots of the secular determinant formed by subtracting E from the diagonal elements of the energy matrix. Resonance occurs when the quantum $h\nu$ equals the difference between the energy levels.

To illustrate this a simple case will be outlined which may be solved exactly. It may be noted that many more complex cases must be solved by numerical methods. Consider the Hamiltonian

$$H_s = \beta \underline{S}.g.\underline{H} + D(S_z^2 - \tfrac{1}{3}S(S+1)) \qquad 3.8$$

where S = 1. The case where the magnetic field is parallel to the D axis will be considered. For this, 3.8 may be rewritten:

$$H_s = g_z \beta H_z S_z + D(S_z^2 - \tfrac{2}{3}) \qquad 3.9$$

Using the standard rules for quantum mechanical operators the energy matrix becomes

	$\lvert 1\rangle$	$\lvert 0\rangle$	$\lvert -1\rangle$
$\lvert 1\rangle$	$g_z\beta H + \tfrac{1}{3}D$	0	0
$\lvert 0\rangle$	0	$-\tfrac{2}{3}D$	0
$\lvert -1\rangle$	0	0	$-g_z\beta H + \tfrac{1}{3}D$

3.10

Subtracting E from the diagonal elements of 3.10 gives the secular determinants which may be solved to yield the energy levels: $\frac{1}{3}D \pm g_z\beta H$, $-\frac{2}{3}D$. The allowed transitions, when $\Delta M_s = \pm 1$ occur when $h\nu = g\beta H \pm D$, assuming D is small compared with $g\beta H$.

3.5 Relaxation Processes

Throughout the foregoing the resonance phenomenon itself has been assumed. That energy can be absorbed by an unpaired spin in a magnetic field to transfer it to another Zeeman level requires that there will be a difference in population between the upper and lower energy levels. This requirement in turn implies the existence of a relaxation process between the spin system and the lattice, because before the field was applied the spins were randomly oriented, having no axis of quantization. When the field is applied only certain orientations are allowed and the spins must initially take up all of these with equal probability. Relaxation to thermal equilibrium will involve some of the spins transferring to the lower energy levels with a characteristic time T_1 known as the spin lattice relaxation time. The phenomenological equations of Bloch (18) require there to be in addition a second relaxation time T_2 which determines the transverse relaxation between the spins. In other words it describes the rate at which energy is transferred between spins. The total Zeeman energy is unaltered by relaxation processes of this kind, whereas it appears as heat (lattice vibrations) in the case of spin lattice relaxation. Since the spin lattice relaxation time determines

how quickly the spins may return to the ground state, it will limit the rate that power may be absorbed before saturation of the transition occurs. If saturation takes place, broadening of the transition will also occur because the central part of the line will suffer loss of transition probability at an earlier stage than the wings, resulting in a widening of the half intensity points of the absorption. The separation of the maxima of the derivative of absorption, which is normally detected, will also be enlarged. In the absence of saturation the spin spin relaxation time will generally determine the linewidth, unless the resonance is lifetime broadened. These conditions are usually readily recognizable in experimental situations. If saturation broadening is occurring, then the linewidth will be reduced by reducing the microwave power incident on the cavity. If the spin spin relaxation time is the broadening mechanism then the linewidth will be independent of power level and temperature. There are other broadening mechanisms with this characteristic however, for example strain broadening (19). If the resonance is lifetime broadened, the linewidth will be reduced by lowering the temperature until some other mechanism dominates. In all the resonance spectra examined in the course of this work there was evidence of lifetime or spin lattice broadening at room temperature, with the exception of the F^+ spectrum in calcium oxide which had the unusually small linewidth of 0.017 gauss at room temperature, and showing no reduction upon lowering to $77^{\circ}K$. That this resonance had a long spin lattice relaxation was demonstrated by the difficulty of preventing saturation at room temperature, and the

impossibility of detecting it at $4^{o}K$, due presumably to saturation beyond detection at the lowest possible power levels available. It is assumed that this small linewidth was due to spin spin relaxation, which would be long in the case of these crystals because of the low concentration of magnetic ions and nuclei. It is unlikely to be a result of the inevitable strains and spreads in crystal fields due, for example, to dislocations, as single electron F centre spectra g values appear to be extremely insensitive to crystal field symmetries as is shown by the F_c^+ centre in calcium oxide (20). This centre consists of one electron trapped at adjacent anion and cation vacancies. The g value of this centre is 1.9995 in powder compared with 2.0000 for the simple F^+ centre. This indicates that even with a strong axial field present, little shift of the line is observed. If there were a spread of g values due to inequivalent sites, it might be expected to be small, therefore the broadening mechanism is almost certainly spin spin relaxation via dipolar coupling to other magnetic centres.

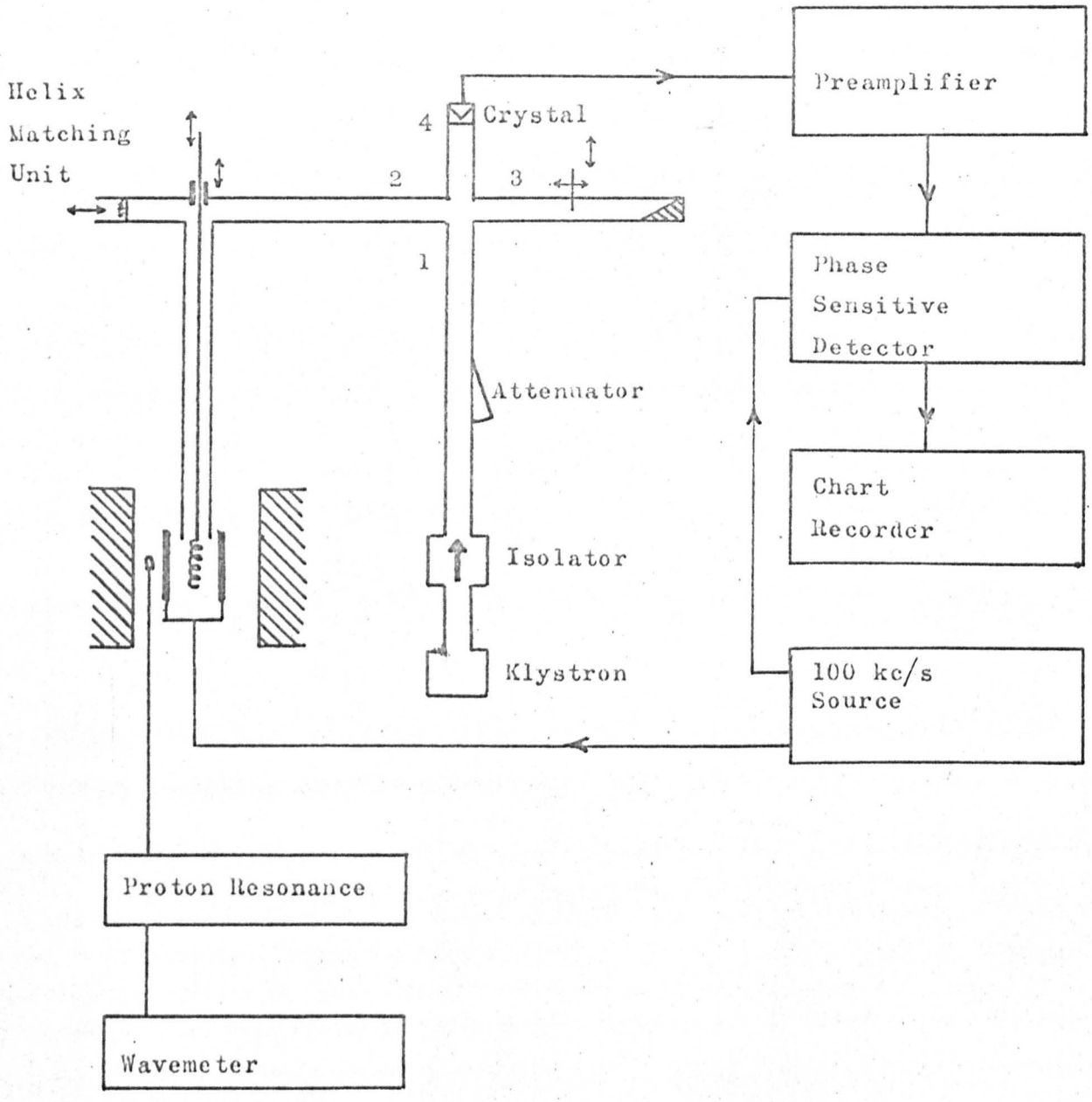

Figure 4.1. The helix spectrometer, operating at X band. Power supplies are not shown, nor are the 50c/s sweep facilities. The unlabelled items in arm 3 of the Magic Tee are firstly a slide screw tuner, and secondly a matched load.

CHAPTER IV

ELECTRON SPIN RESONANCE INSTRUMENTATION

The spectrometers used in the work reported in this thesis were conventional X band (i.e. about 9.2kMc/s) instruments. Two spectrometers will be described in outline, the first a spectrometer employing a helix in place of the more usual resonant cavity, which was used for all the work on silver halides, and a small part of the work on calcium oxide. The second was a commercial instrument, the Varian V4502, used for the majority of the work on calcium oxide.

4.1 The Helix Spectrometer

The helix spectrometer is shown in diagram 4.1. A Varian VA232 klystron supplies about 200mW to arm 1 of the Magic Tee via an isolator and calibrated variable attenuator. The properties of the Tee are such that power incident from arm 1 is divided equally into arms 2 and 3. The slide screw tuner in arm 3 is made non reflecting and all power in this arm is absorbed in the load. A balance is obtained by adjusting the three variable parameters of the helix matching unit shown. These are the position of the variable short, the depth of the stub in the guide and the position of the helix relative to the end of the coaxial line. This balance is detected as a null in the crystal current, as a result of another property of the Magic Tee, that the out of balance power reflected from either arm 2 or 3 is divided equally into arms 1 and 4.

Power in arm 4 is detected by the D.C. crystal current. When a balance has been obtained a small amount of unbalance is introduced by the slide screw tuner to bias the crystal into the non-linear region of its characteristic for efficient detection. The optimum amount of power is in the region of 0.5 to 1.0mW, which effectively puts a lower limit on the amount of power incident on the helix, because there is equal power in arms 2 and 3. This is a grave limitation when studying easily saturable spectra such as that from the F centre in CaO.

Magnetic field modulation is provided at 100kc/s and hence the reflected power on resonance is detected at this frequency at the crystal, which enables a large amount of the $^{1}/f$ noise characteristic of microwave diodes to be eliminated. The preamplifier, a Brookdeal model IA350 had variable high and low pass filters enabling narrow band amplification to be achieved. The gain of 100dB was sufficient to drive the phase sensitive detector, a Brookdeal model PP313A, which when supplied with a reference of suitable phase, and frequency that of the magnetic field modulation, gives a first derivative output of the imaginary part of the susceptibility, provided the field modulation amplitude is smaller than the linewidth. Further discussion of the amplitude and frequency modulation broadening of E.S.R. lines is presented in section 4.3.
The susceptibility is given by $\chi = \chi' - i\chi''$. The purely imaginary part was detected provided the slide screw tuner was adjusted to give maximum crystal current and minimum noise, otherwise a mixture of χ' and $i\chi''$ was

detected. With this spectrometer it was not found possible to detect pure dispersion or χ'. The preamplifier could be made sufficiently wideband to observe spectra by crystal video when used in conjunction with 50c/s magnetic field modulation of amplitude larger than the linewidth, to provide a repetitive timebase.

The helix and its matching circuit is relatively broadband compared with the resonant cavity and hence no microwave locking system was used on this spectrometer. For low temperature measurements a silica sheath was placed round the helix and the whole coaxial line and matching unit evacuated. Field modulation was applied outside the dewar in which the helix was placed, little attenuation resulting from the silvering. Irradiation studies were particularly easy with this arrangement, the helix unit being placed in a thermal bath at the required temperature, and irradiating through the sides. To give good thermal contact with the bath, air was allowed to fill the silica sheath.

The klystron was powered by a Hewlett Packard 716B power supply and the spectra recorded on a Toa EPR-2TB recorder through time constants of up to 10 seconds. The magnetic field was supplied by a Newport Type E 7" air cooled electromagnet powered by a Newport D104 supply. Magnetic fields were measured with a proton resonance unit whose frequency was measured by a heterodyne frequency meter type CKB-74028 and g values measured by comparison with known samples such as DPPH.

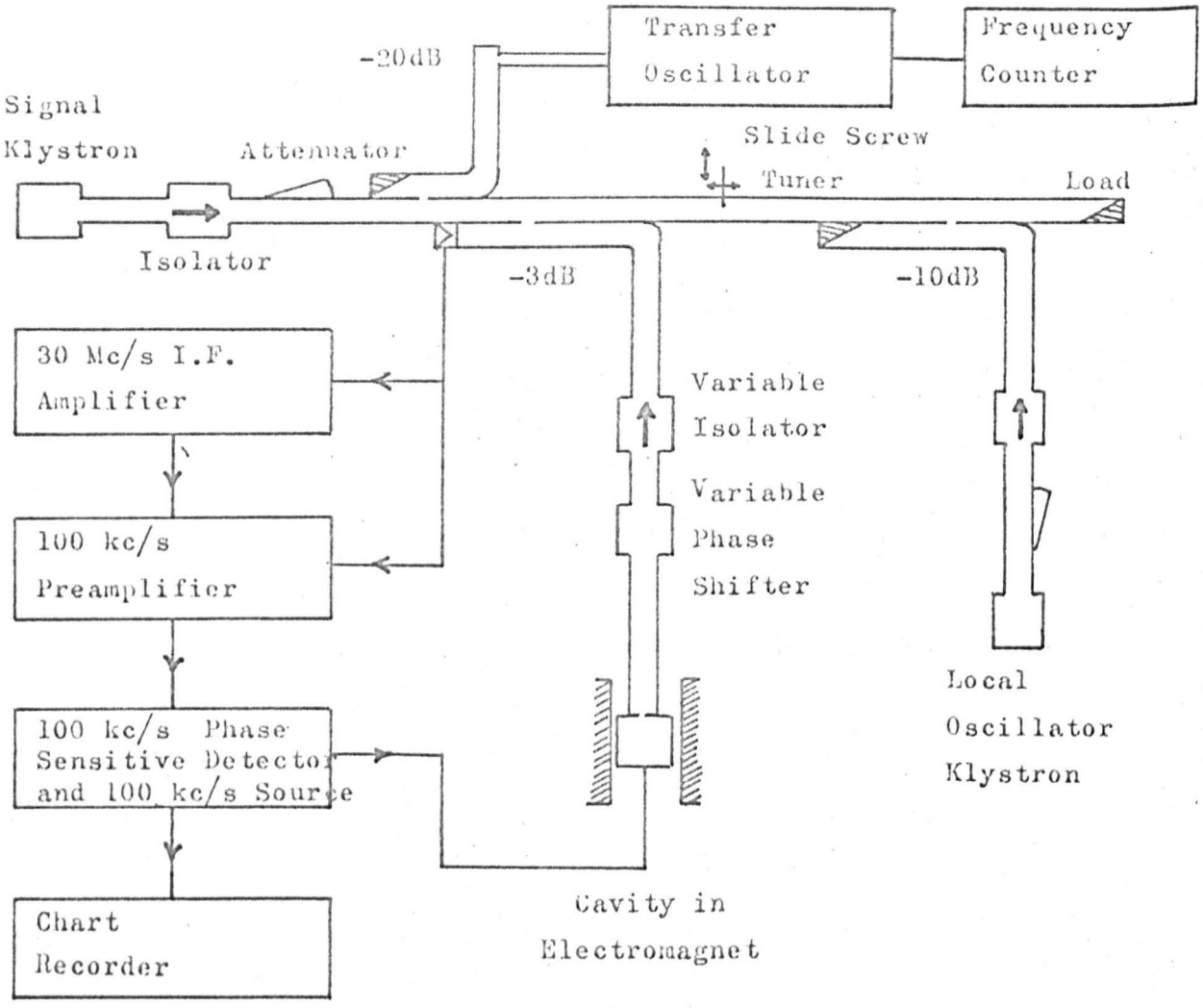

Figure 4.2. The Varian V4502 superheterodyne spectrometer, operating in the configuration used for the present work, at X band. Power supplies are not shown, nor are low frequency and video facilities.

4.2 The Varian V4502 Spectrometer

The Varian V4502 superhet spectrometer is shown in the layout used in Figure 4.2. Power from a Varian V153C klystron is fed via an isolator and variable attenuator to a 20dB coupler. The power in this arm is applied through a coaxial line to a Hewlett Packard 540B transfer oscillator, which enables the microwave frequency to be measured directly on a Hewlett Packard 524D counter. The majority of the power is fed to the 3dB coupler which is equivalent to a Magic Tee. One half of the power goes via a variable isolator and phase shifter to the resonant cavity. The purpose of this isolator is to attenuate power going to the cavity, but not that reflecting back, thereby aiding the study of easily saturable samples. The other half of the power is absorbed in a load, except a small amount reflected by the slide screw tuner to bias the detector crystal. The reflected signal from the cavity is detected at this crystal, and for homodyne operation, amplified and detected in the phase sensitive detector in the usual way. Field modulation and detection were available at 100kc/s and low frequencies from 20c/s to 400c/s, but this latter facility is not shown in the figure.

For superhet operation a second klystron is used for local oscillator power. This is fed via an attenuator, isolator and 10dB coupler into the slide screw tuner arm. The slide screw tuner is not used and the local oscillator power biases the crystal, enabling signal powers down to about 10^{-6} watts to be used. Mixing of the signal frequency and local oscillator frequency occurs at the crystal, and the 30Mc/s

difference frequency is narrow band amplified and detected for the second time. The output is again at 100kc/s or a low frequency and is phase sensitive detected and fed to a chart recorder. Integrating time constants of between 10^{-3} and 10 seconds were available.

Two cavities were used with this spectrometer. The first was a cylindrical H_{012} cavity with Q factor ~ 20,000. Modulation coils were rotated with the magnet facilitating angular dependence studies. For studies involving photoexcitation a rectangular H_{012} cavity was used with a Q factor ~ 7,000. Slots were machined in the end of this cavity to allow illumination during recording. These slots were beyond the cut off frequency for the microwaves. The modulation coils were fixed in the side walls of this cavity preventing the use of the rotating base magnet. Angular variations were plotted by rotating the crystal in the cavity.

Both cavities could be used with suitable cold finger dewars, and low temperature work was carried out at $77^{o}K$ and $4^{o}K$. In the nature of the cold finger dewar system, the crystal temperature was always above that of the liquid coolant, but no attempt was made to measure the actual temperatures. Some work was also carried out using a variable temperature system employing a flow of cooled nitrogen, enabling temperatures between $77^{o}K$ and room temperatures to be held constant. The gas was passed through a heat exchanger in liquid nitrogen and then through a vacuum insulated insert in the cavity. Temperatures were determined by the rate of gas flow, and were measured using a thermocouple mounted by the crystal.

The magnetic field is provided by a 9" water cooled Varian electromagnet powered by a Varian Fieldial controlled power supply. This device consists of a Hall probe in the magnetic field which gives a field proportional voltage when a current is passed through it. Suitable feedback enables preset fields and field sweep rates to be obtained. In practice the linearity has been found to be better than 1% ± 1 gauss, which considerably helps angular rotation studies. The E.S.R. parameters were obtained by calibrating the field with the $M_s = \frac{1}{2} \rightarrow -\frac{1}{2}$ transitions of Mn^{2+} in CaO, for which the parameters are well known, and using the counter to measure the klystron frequency directly.

4.3 Instrumentational Errors

The accuracy of measurements depends on the linewidths and splittings involved which are sample dependant. Instrumentationally the largest errors arise from non linearities of the magnet field sweep, which are most acute on slow sweeps over small field ranges. Except where otherwise stated g value measurements are accurate to 5 in the fifth significant figure and other parameters accurate to 1% or 0.1 gauss, whichever is the larger.

The linewidth which is measured on the chart or oscilloscope may not be the actual linewidth of the transition for the operating microwave power and sample temperature. Beside the sample dependant linewidth, e.g. from spin spin interactions and strain, the detecting

system itself may contribute to the linewidth, and also in some circumstances distort its shape considerably. One of the most important effects arises from magnetic field modulation at high amplitudes and frequencies in order to obtain maximum sensitivity. These two effects will be discussed in turn, but it must also be mentioned that if the homogeneity of the magnetic field H_o is not better than the linewidth over the sample volume then this also will give rise to line broadening. Normally this is only of paramount importance in high resolution nuclear magnetic resonance, but in the case of the very low linewidths of spectra from the F^+ centre in calcium oxide, magnetic field homogeneities of a few parts in 10^6 were necessary, which were met satisfactorily for the Varian 9" magnet.

Since the microwave diodes frequently employed for detection in E.S.R. spectrometers display predominantly a $1/f$ noise characteristic, it is advantageous to detect at high frequencies. The value of 100kc/s is often chosen as offering a compromise of high enough frequency to render the $1/f$ noise comparable with klystron noise, and yet retain conventional audio techniques. In both spectrometers discussed, the 100kc/s mode of operation was the most sensitive and thus most used. The signal was obtained at 100kc/s by modulating the magnetic field with small coils in the air gap. This technique results in a differential of the line being produced when used in conjunction with a phase sensitive detector. The principle is that the modulation amplitude is small compared with the

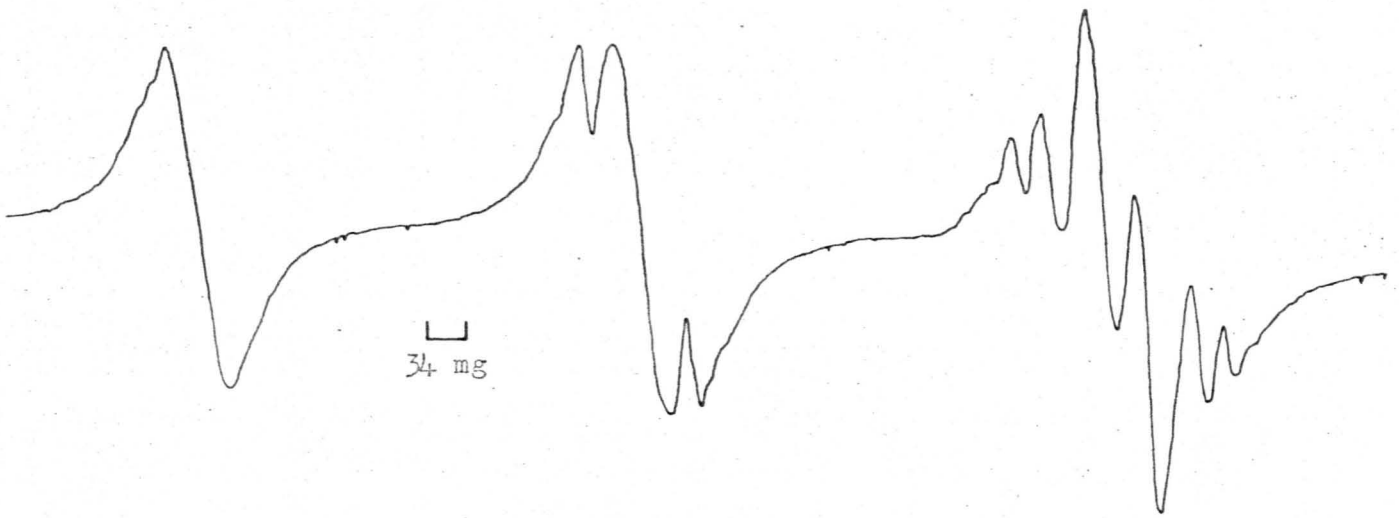

Figure 4.3. 100kc/s modulation sidebands on F^+ centre line. Left hand line was taken with about 40 milligauss (mg) modulation and this amount is doubled successively to the right.

linewidth and that many cycles occur within the time taken to scan the line. It can be shown that maximum line amplitude will occur when the modulation amplitude is approximately equal to the linewidth at half height (21, Chapter X). This then is the condition for maximum sensitivity, but results in distortion of the lineshape, the original condition of small modulation amplitude to linewidth ratio being necessary for true lineshapes to be obtained. If the modulation amplitude becomes large compared with the linewidth, broadening of the observed line occurs. The observed linewidth is nearly proportional to the modulation amplitude. This condition is frequently met with as spectrometers commonly provide a few tens of gauss of modulation, and lines may be considerably less than this in width.

A second type of modulation broadening may occur which is less commonly met. This occurs when the modulation frequency is comparable with or greater than the linewidth, in units of frequency. The effect manifests itself as a series of sidebands centred on the resonance line, and separated by the modulation frequency. The sidebands extend over a range comparable with the peak to peak modulation amplitude, and their relative amplitudes are given by a set of Bessel functions (21, Chapter X). For certain modulation amplitudes the central line will disappear. A few examples are shown in Figure 4.3, the last showing the two lines adjacent to the centre line more prominant than the centre line itself. It has been found, however, that provided the usual condition that the modulation

amplitude is small compared with linewidth is adhered to, the sidebands are negligibly small and the linewidth no greater than with much lower frequency modulation. This was checked by measuring the linewidths of the F^+ centre in calcium oxide using both 100kc/s modulation which gives sidebands for large amplitudes at $\pm$ n x 0.034 gauss and using 400c/s modulation which hypothetically gives sidebands at $\pm$ n x 0.00014 gauss. In each case the result was the same, that the peak to peak derivative width was 0.017 $\pm$ 0.002 gauss. The lineshape was not appreciably different. This result is of some importance as it would not have been possible to observe the hyperfine structure of the F^+ centre, in these crystals with the naturally occurring nuclear isotopes without the sensitivity of the 100kc/s field modulation facility. In practice the central line was observed on the oscilloscope and the modulation intensity increased until the first pair of sidebands could be seen, then the modulation was reduced slightly. This gave best resolution, and almost the best signal to noise ratio.

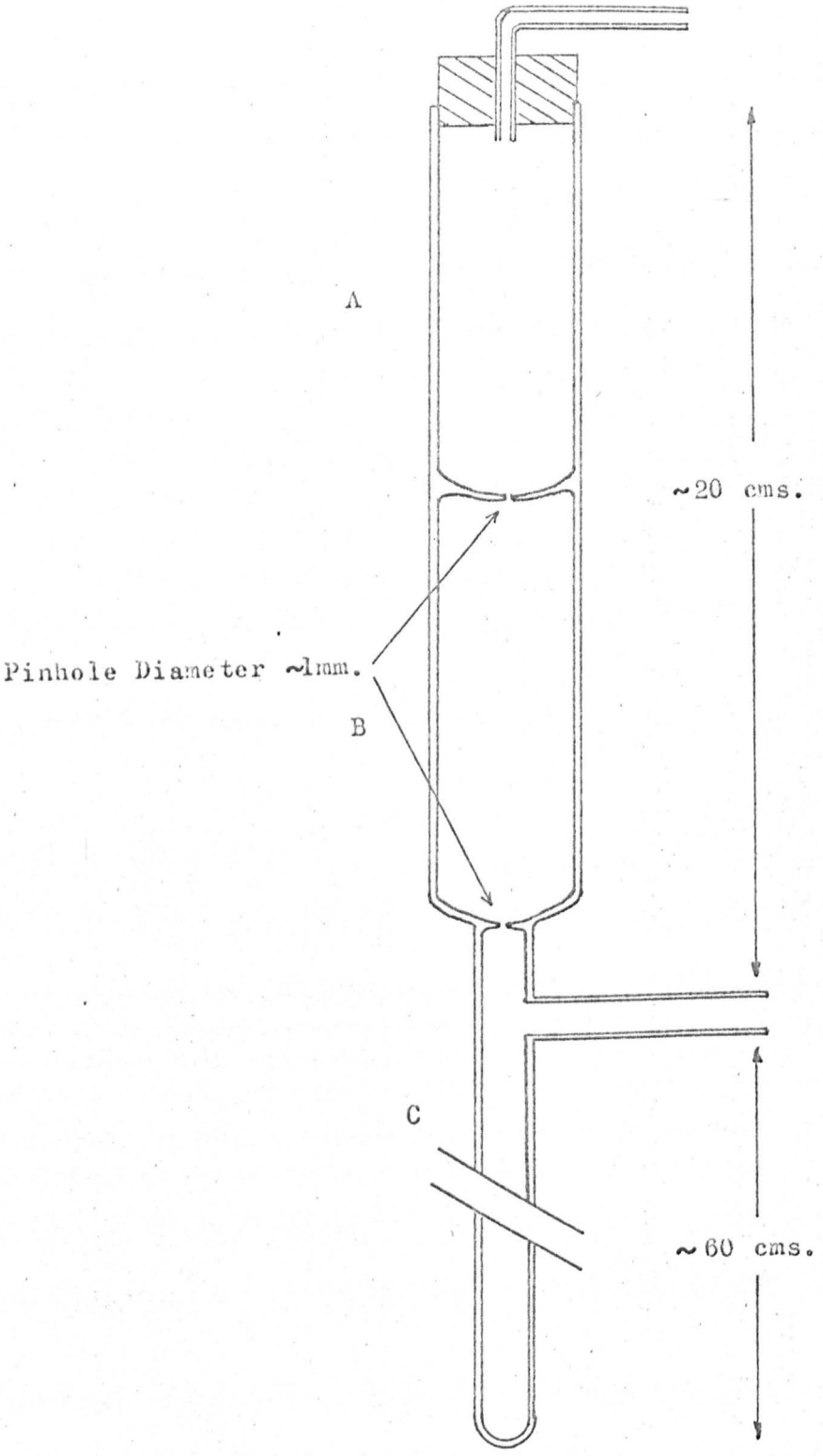

Figure 5.1. Pinholing Apparatus constructed from silica tubing. Powder is packed in A, melted then passed into B. Halogen gas is bubbled through the melt for 20 minutes, then it flows into C where it solifies in ingots suitable for zone refining.

CHAPTER V

CRYSTAL PREPARATION

The techniques used in the handling of the silver halides have very little in common with those used for the simple oxides. Therefore this chapter will be divided into two parts, the first part dealing with the silver halides and the second with calcium oxide.

5.1 Preparation of Silver Halides

Silver chloride and bromide were both produced by the methods outlinedbelow, although for simplicity the description will be confined to silver chloride. Some silver bromide powder of very high purity was supplied by F. Moser of Eastman Kodak Research Laboratories. An analysis of this showed only iron present at less than 0.2p.p.m. Tests were also made for other transition metals but not detected at the threshold of 0.1p.p.m.

Approximately N/5 solutions of silver nitrate and hydrochloric acid were mixed at 50ml/min in excess acid at 70°C. Excess liquid was decanted from the heavy precipitate of silver chloride, and the latter was then washed repeatedly at the completion of the reaction with de-ionized water. The dried powder was packed into the upper part, A, of a pinholing apparatus shown in Figure 5.1 (22) and melted with a gas torch in a halogen atmosphere. By a suitable reduction in pressure the melt was made to flow through the upper pinhole into chamber B.

Deposits of silver and silver oxide were left adhering to the silica walls of A. In chamber B, halogen gas was passed upwards through the melt to convert any remaining silver to the halide. The melt was then allowed into chamber C where it solidifed.

The solid was then zone refined (23) in high purity silica tubing in a horizontal position, with between 80 and 100 zone passes. The central half of the zone refined ingot was used for crystal growing. Crystals were grown in high purity silica tube, which had been flame cleaned, by the Bridgman-Stockbarger technique. By this method the molten silver chloride, under a controlled atmosphere, is slowly passed from a zone of high temperature to a zone of lower temperature below the melting point. If the container has a sharp lower point, which is allowed to cool first, a seed crystal will form there, upon which the whole crystal orientation will depend, provided the solid-liquid interface moves sufficiently slowly to prevent further seeding. In the author's case, the tube containing the melt was firmly mounted on a steel framework to prevent vibration. A small electric furnace, and a water cooled jacket, separated by a mica baffle, were electrically driven up the tube at <1mm/hour. The required doping was added as the anhydrous transition metal chloride, or for low doping, ~ 10p.p.m., a piece of previously doped crystal was added.

Initial orientation of the crystal has been achieved by growing epitaxial sodium chloride crystals on the surface from a saturated solution. An examination can then be made under low magnification for

crystal perfection. Multicrystal growth and even low angle grain boundaries > 1^{o} can be detected using reflected light from a point source. Since no cleaving is possible with the silver halides the crystals have been cut with a stainless steel saw using xylene as a lubricant. The surface damage is removed with a fine carborundum paper using water as a lubricant. Finally 0.5mm of material is removed by etching in 3N sodium thiosulphate. This was followed by a thorough washing, which is particularly necessary where annealing processes are to be used. All the procedures after the crystal growth have been carried out in subdued light, but with the exception of copper doped silver bromide, no significant effects have been observed if full daylight has been allowed to fall on the samples.

Final orientation has been achieved by using the anisotropic behaviour of the E.S.R. spectra of the $^{6}S_{5/2}$ ions Fe^{3+} or Mn^{2+} at $77^{o}K$. The linewidths and resolution of the transferred hyperfine interaction in the case of Fe^{3+} were taken as indicators of the degree of imperfection of the crystal. In a good sample the linewidth of individual hyperfine components of the $M_s = \frac{1}{2} \rightarrow -\frac{1}{2}$ transition were smaller than the splittings.

Annealing studies were performed by sealing cut and etched samples in high purity quartz tubes in controlled atmospheres and heating in a thermostatically controlled electric furnace. Irradiation studies were made using the filtered output of a high pressure mercury lamp. In practice filtering was found to have little if any effect on the E.S.R.

spectra or the degree of surface darkening. The temperature of irradiation was obtained by immersing the E.S.R. helix containing the crystal in various coolants, and the temperature monitored with a thermocouple.

5.2 Preparation of Calcium Oxide

The calcium oxide crystals were grown by the arc fusion method by Muscle Shoals Ltd., Alabama. They were kindly supplied to the present author by Dr. B. Henderson, Keele University. The arc fusion method of crystal growth gives very poor control over crystal purity, because several kilograms are required for each melt, and highly pure powder is prohibitively expensive. Furthermore impurities are electrolytically introduced from the carbon electrodes. Briefly, two electrodes are placed in a mass of powder and an arc struck between them. The powder near the electrodes melts and then cools slowly when the arc is cut off. Single crystals of up to 1cm side length are formed as a result in calcium oxide (rather larger for magnesium oxide). It is evident from observations made on some of these crystals that electrolytic reduction can take place near the electrodes, as some samples taken from near the electrodes were inhomogeneously coloured brown, similar to crystals annealed in metal vapour (9). It is assumed that the oxygen had reacted with the carbon electrodes.

The crystals cleave preferentially along {100} planes making orientation extremely simple. Pieces approximately 5 x 3 x 2mm were used

in the E.S.R. experiments, and final orientation was checked using the E.S.R. of Gd^{3+} which has a reasonably large fine structure splitting. Irradiation at 77°K was carried out in the cold finger dewar used for E.S.R. studies at that temperature. Some sample temperature rise must have occurred but this was not monitored. Generally the unfiltered output of a high pressure mercury lamp was used, but for the observation of transient spectra filtering was achieved when required with Kodak Wratten filters. This enabled the optical absorption band associated with the defect giving the E.S.R. spectrum to be identified. Some crystals were annealed in air by suspending them on platinum wire in a thermostatically controlled electric furnace. Annealing up to 1300°C was possible by this method. The crystals were quenched by bringing them directly into the room or slow cooled by a temperature/time programme on the furnace control.

CHAPTER VI

SILVER HALIDES : RESULTS AND DISCUSSION

6.1 AgCl:Fe; AgBr:Fe.

Iron can dissolve in silver chloride and bromide in the divalent or trivalent state. In a neutral atmosphere (e.g. vacuum) the divalent state appears to be in equilibrium in the dark at all temperatures below the melting point. In an oxidizing atmosphere (the halogen gas) the trivalent state is preferred at sufficiently high temperatures for efficient ionic diffusion.

Although E.S.R. due to Fe^{2+} in AgCl and AgBr have not been detected, optical spectra (24) and Mossbauer spectra (25,26) suggest that Fe^{2+} is on a silver ion lattice site, with a tetragonal distortion, assumed due to a charge compensating silver ion vacancy in a next nearest neighbour position along the 100 direction. E.S.R. spectra have been reported from Fe^{3+} in both AgCl and AgBr (14). The Fe^{3+} was found to be in an interstitial site with four tetrahedrally coordinated halide ions, and four neighbouring silver ion vacancies. The overall $(FeX_4)^-$ complex (where X is a halide ion) is negatively charged, but shows cubic symmetry indicating the charge compensation occurs remote from the complex. The E.S.R. spectrum of Fe^{3+} (which is a $3d^5$, $^6S_{5/2}$ ion) in a cubic environment has been fitted to the Spin Hamiltonian:

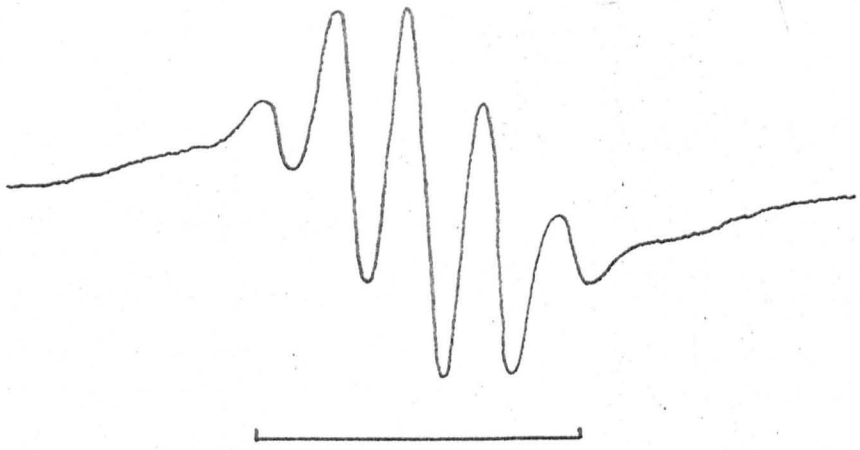

Figure 6,1. E.S.R. spectrum of Fe^{3+} in AgBr:Fe produced by optical irradiation at temperatures between 153°K and 186°K. Recorded at 77°K.

Table 6.1. Parameters of the spin Hamiltonians of Fe^{3+} in AgCl and AgBr at 77°K. Fine structure terms in units of 10^{-4} cm^{-1}.

Complex	g	a	D	F	Ref.
$(FeCl_4)^-$	2.0156 ±.0004	75.0 ±0.3	-	-	(14)
$(FeCl_4)^-Ag^+$	2.0063 ±.0010	181.0 ±1.0	81.3 ±1.0	6.3 ±1.0	(28,30)
$(FeBr_4)^-$	2.045 ±.005	?	-	-	(14)

$$H_s = g\beta H.S + \frac{a}{6}\{S_x^4 + S_y^4 + S_z^4 - \frac{1}{5}S(S+1)(3S^2+3S-1)\} + \sum_n H_N^n \qquad 6.1$$

The first term is the Zeeman effect ($S = 5/2$), the second the crystal field splitting term and the third describes the effect of the transferred hyperfine splitting due to the ligand halogen ions. In each case the transferred hyperfine splitting was only detected on the $M_s = \frac{1}{2} \leftrightarrow -\frac{1}{2}$ transition, and in AgBr only this transition was detected at all, the others were presumed broadened beyond detection by lattice defects (14). This lead Hennig (27) to suggest that the defect had $S = \frac{1}{2}$, and he proposed a hole trapped at a positive ion vacancy. However this may be discounted for the following reasons: Hayes and the present author have failed to produce this spectrum in nominally pure AgBr crystals (Fe content < 1p.p.m.), under identical conditions to those under which the spectrum is produced in iron doped crystals; secondly the precise antimorph of the F centre is not likely to form a stable complex, but a trapped hole would more probably appear as a molecular complex as in the alkali halides. This production of the spectrum may most reasonably be attributed to residual iron impurity.

The method used to produce the spectra attributed to $(FeX_4)^-$ was annealing in a few atmospheres of halogen gas at temperatures of a hundred degrees or so below the melting point of the crystal. This was followed by rapid quenching to 77^oK. This procedure has been followed by the present author and the same spectra produced. The parameters are listed in table 6.1. No attempt was made to repeat the analysis of the hyperfine interaction.

Hay (28,29,30) found that it was possible to produce the identical spectrum in AgCl:Fe^{2+} by irradiation from a filtered high pressure mercury lamp. In this case the temperature range over which the spectrum was produced was between 200°K and 273°K. Lowering the temperature of irradiation to between 178°K and 200°K resulted in no spectrum being formed, but between 168°K and 178°K a new $^6S_{5/2}$ spectrum was produced which has been fitted to the spin Hamiltonian:

$$H_s = g\beta H.S + \frac{a}{6}\{S_x^4 + S_y^4 + S_z^4 - \frac{1}{5}S(S+1)(3S^2+3S-1)\} + D\{S_1^2 - \frac{1}{3}S(S+1)\}$$
$$+\frac{F}{180}\{35\ S_1^4 - 30\ S(S+1)S_1^2 + 25\ S_1^2 - 6S(S+1) + 3S^2(S+1)^2\} \qquad 6.2$$

where x, y and z are the crystal axes and the 1 axis is parallel to a 111 direction. The measured parameters are recorded in the second row of table 6.1. Below 168°K and down to 77°K no spectra were produced, and irradiation was not attempted below this temperature. This second spectrum has been attributed to a trignally distorted tetrahedral $(FeCl_4)^-$ centre, and the model is as for the tetrahedral centre but with one silver ion site occupied. Thus the overall $(FeCl_4)^-Ag^+$ trigonal centre is charge neutral.

If the crystal containing this centre is warmed to 200°K the spectrum is unaltered, but warming above this temperature results in the decay of this spectrum in approximately a 1:1 ratio into the tetrahedral spectrum. This suggests that the thermal energy is sufficient to overcome the electrostatic binding energy of the charge compensating

silver ion. The stability of the tetrahedral $(FeCl_4)^-$ complex depends upon the concentration of iron and the degree of mechanical damage suffered by the crystal. With 10p.p.m. of iron the spectrum may be fairly stable at 373°K, but rapid cycling between room temperature and 77°K would destroy it. With higher iron concentrations the spectrum was seldom stable at room temperature and although the intensity was not usually much greater than with the lower concentration, re-irradiation following decay gave nearly the same intensity again in contrast to the lower concentrations which only gave weak spectra on subsequent irradiation. This suggests that some of the iron at least was "used up" in this irradiation-decay process. It is probable that thermal decay is associated with migration of the complex through the crystal to dislocation lines, where Fe^{2+} or Fe^{3+} may become permanently trapped (31).

It has also been found possible to produce the tetrahedral $(FeBr_4)^-$ complex by visible radiation, in this case over the temperature range 153°K to 186°K. The spectrum from this radiation produced centre is shown in Figure 6.1, and is identical to the spectrum published by Hayes. Irradiation between 77°K and 153°K produced no other spectrum, hence the equivalent trigonal spectrum in the bromide is either not stable above 77°K or it is weak and broadened beyond detection.
The tetrahedral spectrum was found to be stable up to 343°K when typically it decayed in twenty minutes to half intensity. However, the concentration and damage dependance of the stability of the spectrum was more marked in

AgBr than in AgCl. Reproduction of the spectrum by re-irradiation following decay was generally poor. Irradiation above 193°K bleached the spectrum, which is a considerably lower temparature than that at which thermal decay occurred for any sample.

Evidently Fe^{2+} in the silver halides can act as a hole trap in certain circumstances. The mechanism proposed by Hayes for hole trapping in the halogen gas was firstly absorption of a halogen molecule on the surface, as ions, releasing two holes into the crystal. These diffuse through the crystal and are subsequently trapped at Fe^{2+}, which on becoming Fe^{3+} jumps into the interstitial site. The silver ions diffuse away and eventually form more crystal material by joining the adsorbed halide ions on the surface. Various alternative details of the mechanisms are equally plausible.

The mechanism for formation of centres by radiation must clearly be different as there is no source of free halogen. It is proposed that the radiation ejects electrons from the X^- ions, creating electron hole pairs. Holes are trapped by Fe^{2+} and thus the complex is formed. The silver ions (one for the trigonal centre, two for the tetrahedral centre) migrate away. The fate of the electrons must be considered and in AgCl:Fe it is reasonable to suppose that at least two processes are operating in the different temperature ranges. In this case below 168°K, Fe^{2+} ions may act as recombination centres, hole trapping followed by electron trapping. Between 168°K and 178°K

some other electron trap must be operative to allow the formation of the trigonal centre, but this must be thermally unstable above 178°K. A possible candidate would be an interstitial silver ion. Thus above 178°K up to 200°K, Fe^{2+} again acts as a recombination centre. Above 200°K electrons are again trapped elsewhere allowing the formation of the tetrahedral centre. The most likely trap in this case is silver ions at dislocation jogs (32).

The same mechanism is proposed for the formation of the $(FeBr_4)^-$ centre, but at characteristically lower temperatures for ionic processes in AgBr. Below 153°K, Fe^{2+} acts as a recombination centre, but above 153°K and up to 186°K holes are trapped by Fe^{2+} which moves to the interstitial position followed by the dissociation of the Ag^+ ions; electrons are trapped by Ag^+ ions on dislocation jogs. Irradiation above 193°K resulted in a bleaching of the $(FeBr_4)^-$ spectrum, implying that above this temperature the centre is an electron trap. Re-irradiation at temperatures between 153°K and 186°K following this bleaching reproduces the centre, suggesting that the bleaching process had returned the iron to its original state. This result is surprising as the $(FeBr_4)^-$ complex is negatively charged and should repel electrons. However it must be concluded that the centre is a more efficient trap than the bromine atoms or molecular ions formed by the irradiation. In this reverse process it is proposed that ultimately the holes will be trapped on the Ag^0 atoms that have been found during the photo formation of the $(FeBr_4)^-$ complex.

All attempts to bleach the $(FeCl_4)^-$ complex up to room temperature have failed. Experiments indicate that the stability of this centre is not affected by visible radiation at room temperature.

6.2 AgCl:Mn

E.S.R. spectra have been reported from manganese doped AgCl (33). The manganese ion is divalent and thus isoelectronic with Fe^{3+}. The spectra indicated that at low temperatures the ion was in a cubic environment with an axial distortion in the 100 direction. At room temperature the spectrum was broadened, and consisted of six $M_s = \frac{1}{2} \leftrightarrow -\frac{1}{2}$ hyperfine lines, the fine structure averaged to zero by the hopping of the vacancy from one site to another. In view of the results on trivalent iron, it was thought that it may be possible to obtain tetravalent manganese in the tetrahedrally coordinate interstitial site analogous to $(FeX_4)^-$. Mn^{4+} is a $3d^3$ system and has been studied in other ionic crystals (e.g. 34). Spectra from Mn^{4+} are usually readily detectable. In spite of various heat treatments, principally annealing in about 10 atmospheres of chlorine, followed by quenching, and irradiation studies from 77°K to room temperature, the spectra remained exactly as reported by Schneider and Sircar. The crystals containing about 100p.p.m. Mn were a pale yellow after the anneals.

6.3 AgCl:V

Following the E.S.R. and optical studies of $NaCl:V^{2+}$ (35) an analogous study was proposed for $AgCl:V^{2+}$. Crystals were grown containing

between 1000p.p.m. and 1p.p.m. of anhydrous VCl_2 kindly supplied by Dr. E. Hutchinson, Argonne National Laboratory. The heavily doped crystals were a deep pink, and their zoned growth suggested that these contained considerably more vanadium than was in thermodynamic equilibrium. For the crystal with heaviest doping, a deeply coloured region at the beginning of crystal growth was separated by a pale central region from the final coloured region. This suggests that for a heavily doped melt, an initial reduction in concentration is achieved by precipitation, followed by a near saturation solid solution, and the remainder precipitates in the final region. Unfortunately the E.S.R. spectra were extremely poorly resolved, consisting of a few weak lines superimposed on a very broad background absorption with g = 2.0. The lines could not be grouped into eights as would be expected from the 100% abundant ^{51}V with I = $7/2$.

6.4 AgBr:Cu

The properties of single crystals of silver chloride doped with copper have been extensively studied by E.S.R. as copper is thought to play an important role in the photographic process. The E.S.R. spectra indicated (36) that the copper could exist in two forms dissolved in the crystal, and possibly in addition a third form as aggregated $CuCl_2$. This latter was not fully substantiated by E.S.R. The dissolved copper was either Cu^+ which is diamagnetic or Cu^{2+}. The spectra from Cu^{2+} were obtained after chlorine anneals, and indicated that three inequivalent

sites existed each with axial distortions. Furthermore the hyperfine structure from the isotopes Cu^{63} and Cu^{65} each with I = $^3/_2$ was observed for each of the centres.

It was thought worthwhile to grow crystals of silver bromide doped with copper to see whether comparable results could be obtained. Crystals were grown under inert and brominating atmospheres, and in view of the expected photosensitivity were handled under a safelight at all times. The results obtained, however, were quite unreproducible.

Annealing crystals grown in nitrogen atmospheres or examining bromine grown samples showed no spin resonance spectrum, with one exception; this one crystal which was grown under nitrogen and annealed in bromine, showed a single line spectrum when quenched to 77°K. The resonance was anisotropic with g varying between about 2.0 and 2.2, but unfortunately the resonance decayed before measurements were made. However no hyperfine structure was observed which was surprising as the linewidth of 70 gauss should have allowed at least partial resolution. It is unlikely that this resonance was due to aggregated $CuBr_2$ which may have masked the hyperfine structure, as a much broader line would then be expected as was observed in AgCl.

CHAPTER VII

RESULTS AND DISCUSSION FOR DEFECTS IN CALCIUM OXIDE

7.1 General Remarks on Optical and E.S.R. Spectra

Preliminary investigations of the crystals revealed that inhomogeneous brown colouration was present in some of the crystals, which had, as previously mentioned, been taken from near the electrodes in the melting procedure. E.S.R. spectra showed that the uncoloured regions of the crystals contained the S state ions Gd^{3+} and Mn^{2+}. The coloured regions contained in addition to these ions the ion V^{2+} and the F^{+} centre (consisting of one electron trapped at an oxygen vacancy, see section 2.1 for nomenclature). Each of these defects has been reported previously in calcium oxide (see (11) for the impurity ions and (6) for the F^{+} centre) and thus they will not be discussed in detail at this stage. Optical absorption bands have been reported in calcium oxide at 3.65 and 3.1eV and assigned to the F^{+} and F centres respectively (44,37,8). Since there had evidently been a chemical reduction in the brown regions of the crystal, similar to that caused by annealing oxide crystals in metal vapour (9) it seemed probable that F centres were present as well as F^{+} centres. The F centres may be considered to a first approximation as a helium like centre with $^{1}S_{o}$ ground level which is diamagnetic. No E.S.R. spectrum would be expected from this centre in the ground state.

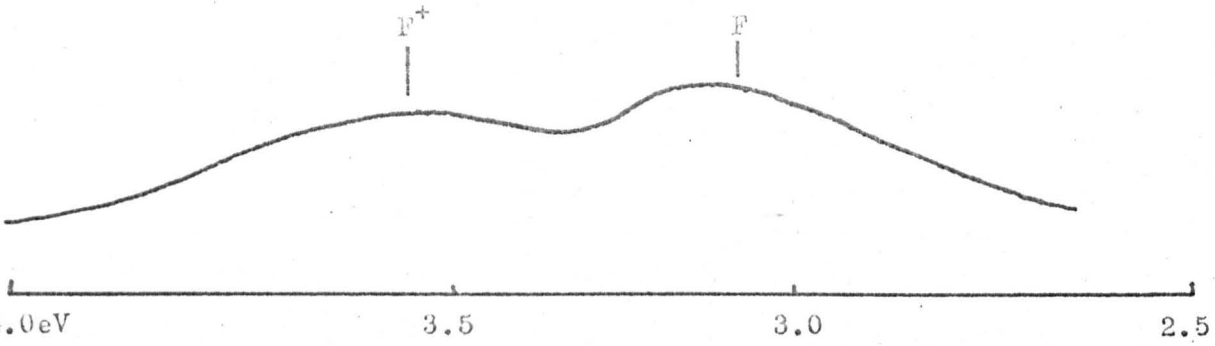

Figure 7.1. Optical absorption spectra of naturally coloured calcium oxide crystals obtained on a UNICAM SP.800 spectrophotometer at 290°K.

Table 7.1. Linewidths of E.S.R. spectra in calcium oxide single crystals in units of gauss. Widths measured on the derivative from peak to peak.

Defect Centre	Crystals as grown		Annealed and slow cooled		Annealed and quenched	
	290°K	77°K	290°K	77°K	290°K	77°K
¡Gd^{3+}	0.8	0.1	0.8	0.8	0.8	0.8
¡Mn^{2+}	0.6	0.1	0.6	0.5	1.0	0.7
¡Fe^{3+}	+	8	+	8	+	12
Cr^{3+}	1	0.2	+	0.5	+	0.7
¡V^{2+}	1	0.15	-	-	-	-
Ti^{+}	1	0.2	-	-	-	-
F^{+}	0.02	0.02	-	-	-	-
V	+	1	+	1	+	1
W	-	-	-	-	+	1.5

¡ Measured on the $M_s = \frac{1}{2} \leftrightarrow -\frac{1}{2}$ transition.

+ Line very broad.

- Defect not detected.

All linewidths measured along a principal axis.

Optical absorption experiments made at room temperature on a Unicam S.P.800 spectrophotometer revealed a strong band peaking at an energy just less than 6eV. Superimposed on this band were two weak bands at 3.6 and 3.1eV which are shown subtracted from the 6eV band in Figure 7.1. Which of these optical bands gives rise to the visible colouration is an open question. The 6eV band was so broad and strong (width at half intensity 1.1eV and absorbance 30 times that of the 3.6eV band) that both the 6eV and the 3.1eV band entered the blue region of the visible spectrum. It is possible that the 6eV band is due in part to the presence of colloid metal. However uncoloured crystals also showed some increase in absorbance in this spectral region, and thus the effect of atmospheric corrosion of the surface may be quite important at these photon energies. Unfortunately the crystals available were insufficiently large to permit the use of freshly cleaved surfaces which would have reduced this problem.

While the existence of colloid metal particles is speculative, the presence of F^+ and F centres seems assured. No E.S.R. due to conduction electrons in the colloid particles was observed, but this is not too surprising as the conduction of divalent metals such as calcium arises from the overlapping of bands, and the resulting paramagnetism may be difficult to detect. No optical absorption bands were detected in the colourless samples.

Thus the brown crystals were found to be strongly reduced chemically and were almost certainly non stochiometric, i.e. contained in

this case more cations than anions. Furthermore many defects were in the most reduced form that was stable at room temperature. Ultraviolet irradiation was able to induce electron transfer among the defects in these crystals however and thus some of the defects could take on more electrons which implies a further chemical reduction.

It is presumed that the proportion of impurities in the two distinctly coloured crystal types was roughly the same, and for example vanadium was present in the colourless crystals as V^{3+} which has not been detected in calcium oxide by E.S.R. When an inhomogeneously coloured single crystal showing spectra due to V^{2+} was cleaved to separate the colourless region, the V^{2+} spectra were only present in the coloured part, but other impurities were present in the same proportion by weight and the low temperature linewidths, probably dependant on the spin spin relaxation time, which is dependant on the concentration of magnetic ions and nuclei, were the same for the ions present in both sections of crystal. There is in any case no a priori reason to suppose the concentration of impurity ions should be substantially different for adjacent regions of the same crystal.

Facilities were not available to check the above arguments by annealing colourless samples in calcium vapour. It is expected the crystals would show all the characteristics of the coloured samples had this been possible. Instead both sorts of crystal were given various heat treatments in oxydizing atmospheres, and provided the treatment was sufficiently strong the same results were obtained for both. Examination

of the E.S.R. spectra of crystals which were originally coloured, which had been annealed at 1300°C for 24 hours in air at atmospheric pressure and then quenched to room temperature in less than one minute revealed the following changes:

$$Mn^{2+} \rightarrow Mn^{2+}$$

$$Gd^{3+} \rightarrow (Gd^{4+}?)$$

$$V^{2+} \rightarrow (V^{3+})$$

$$(Fe^{2+}) \rightarrow Fe^{3+}$$

$$(Cr^{2+}) \rightarrow Cr^{3+}$$

$$\begin{matrix} F^{+} \\ \text{centres} \\ F \end{matrix} \rightarrow \begin{matrix} V \\ \text{centres} \\ W \end{matrix}$$

The crystals were a pale yellow after quenching irrespective of their colour before heat treatment. The bracketed ions were not detected but were the presumed state of ionization taking circumstantial evidence and the known tendencies of some of the transition metal ions into account. The concentration of Mn^{2+} ions was apparently unaltered, suggesting that it was not changed to Mn^{3+}, nor was there any evidence that it had become Mn^{4+}, which has been detected by E.S.R. in calcium oxide (11). Thus it would appear that this chemical state brought on by quenching from 1300°C was not the most oxydized state possible. Higher temperature heat treatment would presumably provide further oxydization. The Gd^{3+} spectrum could not be detected directly after the quenching process, but returned with reduced intensity after a few weeks at room temperature. Fe^{3+} and Cr^{3+} spectra were detected in considerable concentrations, but both

decayed over a period of weeks to low, but detectable values. This phenomenon is similar to, but significantly different from work on colour centres in magnesium oxide produced by X-ray and heat treatment (38). On the whole Fe^{3+} and Cr^{3+} are the favoured ionization states in MgO, but Cr^{3+} is more stable than Fe^{3+}. In calcium oxide, however, the divalent states are more stable, as the trivalent states once formed decay within a period of days or weeks depending on crystal history. The principal reason for the difference in behaviour is most probably explained by the difference in ion sizes: Cr^{3+}, 0.69Å; Fe^{3+}, 0.64Å; Mg^{2+}, 0.65Å compared with: Cr^{2+}, 0.84Å; Fe^{2+}, 0.76Å; Ca^{2+}, 0.99Å.

Following the quenching process the F^{+} centre spectrum was undetectable, and the optical absorption bands at 3.6 and 3.1eV had vanished. Instead spectra due to two types of hole centre were present which will be discussed more fully in section 7.5. Oxidizing heat treatment, which was less strong than quenching from 1300°C after a 24 hour anneal, showed similar effects, but these were less pronounced. Very few V centres were present in quenched crystals which had only been heated for a period of minutes, suggesting that the excess oxygen takes at least a period of hours to diffuse in to equilibrium concentrations. In (38) it was found that the colour centre effects produced by oxidising anneals was proportional to the logarithm of pressure, suggesting an impurity limited process which is in contrast to experimental evidence from halogenating treatment on the alkali halides. This shows a power

dependance on gas pressure indicating that the law of mass action governs the concentration of colour centres. In this case the impurity content is negligible compared with the numbers of V centres formed.

A noticeable feature of the E.S.R. spectra was the small linewidths observed for many of the defects in these calcium oxide crystals relative to linewidths reported in other such crystals (see references in (11)), and in calcium oxide from another melt which the author has subsequently examined. These linewidths are shown in table 7.1 for all defects observed under various conditions in these crystals. The small linewidths are probably due to a combination of circumstances. The most important is certainly a low residual strain in the crystals, which in turn must be due to the very good natural annealing the crystals received as they cooled after the growth stage. This is shown by the fact that the linewidths at $77^{o}K$ in annealed and slow cooled crystals have in general increased. In this case the crystals were cooled at less than one degree absolute per minute. The implication is that the original growth process introduced less strain than any subsequent heat treatment, even that normally expected to reduce strain. The second reason for the small linewidths in these particular crystals is the low concentration of paramagnetic defects, being less than 10^{16} per cubic centimetre for any one species and less than 10^{17} per cubic centimetre overall. More typically the concentration of paramagnetic defects would be two orders of magnitude greater in calcium oxide. In this latter case significant broadening due to spin spin interactions between defect centres may occur even in well

annealed crystals. Finally the low natural abundance of nuclear isotopes of calcium and oxygen with non-zero nuclear spin will reduce the spin spin broadening in all calcium oxide crystals, but probably will seldom if ever be the limiting broadening mechanism in crystals grown by presently available methods. The transition metal ions, in spite of being lower in concentration than the magnetic nuclear isotopes would have a dominant broadening effect because of their considerably larger magnetic moments.

Referring to table 7.1, it can be seen that the linewidths are generally lower at 77°K, indicating that in these cases spin lattice relaxation dominates the broadening at room temperature. Notable exceptions are Gd^{3+} in annealed crystals where strain is presumed the dominant mechanism, and the F^{+} centre where spin spin broadening is assumed the dominant mechanism although magnetic field inhomogeneities may be contributing. The $3d^{3}$ ions Cr^{3+}, V^{2+} and Ti^{+} are notable for their similarity of linewidth. This is probably more pronounced than it appears from the table. The linewidths for Cr^{3+} and Ti^{+} are taken on the line arising from ions with no nuclear magnetic moment, i.e. the central line which consists of three precisely overlapping transitions. This will be broadened by the $M_s = \pm\frac{1}{2} \leftrightarrow \pm 3/2$ transitions which are sensitive to random axial electric fields. In the case of V^{2+} however the eightfold splitting of the line due to the almost 100% abundant V^{51} with $I = 7/2$, gives rise to a second order splitting of the transitions and hence the $M_s = \frac{1}{2} \leftrightarrow -\frac{1}{2}$ transition can be observed independantly.

Some broadening of the other electronic transitions was detected. Thus if the three transitions were overlapping for V^{2+} as in the other $3d^3$ ions it is probable that the linewidths at 77°K would be nearer 0.2 gauss.

7.2 $\underline{Gd^{3+}}$

The E.S.R. spectrum of the $^8S_{7/2}$ ion Gd^{3+} in calcium oxide has previously been reported (39,40). However, linewidths of 17 and 12 gauss respectively at 77°K prevented resolution of the hyperfine structure from the isotopes Gd^{155} and Gd^{157} each of which has a nuclear spin $3/2$. In the present work gadolinium occurred as an accidental impurity in rather low concentrations and the linewidths were two orders of magnitude smaller at 77°K than for the earlier work, making complete resolution possible at this temperature, and partial resolution possible at room temperature.

Using the notation of Baker et al. who investigated the E.S.R. spectrum of $^8S_{7/2}$ ions in the cubic field of calcium fluoride (41) the spectrum may be fitted to the spin Hamiltonian:

$$H_s = g\beta \underline{H}.\underline{S} + B_4(O_4^0 + 5\ O_4^4) + B_6(O_6^0 - 21\ O_6^4) + A\underline{S}.\underline{I} \qquad 7.2a$$

where $S = 7/2$, and $60B_4 = b_4$ and $1260B_6 = b_6$ are the experimentally determined fine structure parameters, and A is the isotropic hyperfine structure parameter relevant when $I \neq 0$. The O_n^m are the spin operators transforming as spherical harmonics, and are listed in detail in the appendix to (41). However, in order to relate this Hamiltonian to the

general Hamiltonian described in Chapter 3 it is worth mentioning that the term $B_4(O_4^o + 5\ O_4^4)$ is equivalent to the cubic term $a/6\{S_x^4 + S_y^4 + S_z^4 - \frac{1}{5}S(S+1)(3S^2+3S-1)\}$ in equation 3.5 with $a = 120B_4 = 2b_4$. Using the operators defined in (41) an analogous expression may be derived for the sixth order term B_6. This Hamiltonian yields three zero field energy levels, neglecting hyperfine interaction:

$$\begin{aligned} \Gamma_6 \text{ doublet} &: E = 32b_4 - 8b_6 \\ \Gamma_8 \text{ quartet} &: E = 20b_4 + 28b_6 \\ \Gamma_7 \text{ doublet} &: E = 0 \end{aligned} \qquad 7.2b$$

The energy matrix factorises exactly for the condition that the magnetic field is directed along a principal axis, and the eigenvalues are given by:

$$\begin{aligned} E_{\pm 7/2} &= \frac{52b_4 + 20b_6 \pm 3G}{2} \pm \tfrac{1}{2}\{(12b_4 - 36b_6 \mp \tfrac{2G}{3})^2 + \frac{140G^2}{9}\}^{\frac{1}{2}} \\ E_{\pm 5/2} &= \frac{20b_4 + 28b_6 \pm G}{2} \pm \tfrac{1}{2}\{(20b_4 + 28b_6 \mp 2G)^2 + 12G^2\}^{\frac{1}{2}} \\ E_{\pm 3/2} &= \frac{20b_4 + 28b_6 \mp G}{2} \pm \tfrac{1}{2}\{(20b_4 + 28b_6 \pm 2G)^2 + 12G^2\}^{\frac{1}{2}} \\ E_{\pm \frac{1}{2}} &= \frac{52b_4 + 20b_6 \mp 3G}{2} \pm \tfrac{1}{2}\{(12b_4 - 36b_6 \pm \tfrac{2G}{3})^2 + \frac{140G^2}{9}\}^{\frac{1}{2}} \end{aligned} \qquad 7.2c$$

where $G = g\beta H$. Note the error in equation 19.5 on page 115 of (42). For the even isotopes the spectrum consists of seven lines corresponding to the $\Delta M_s = \pm 1$ transitions. The spectrum is symmetrical about the $M_s = \frac{1}{2} \leftrightarrow -\frac{1}{2}$ transition, which is most intense and has a smaller linewidth by a small margin. The fine structure parameters are found to be

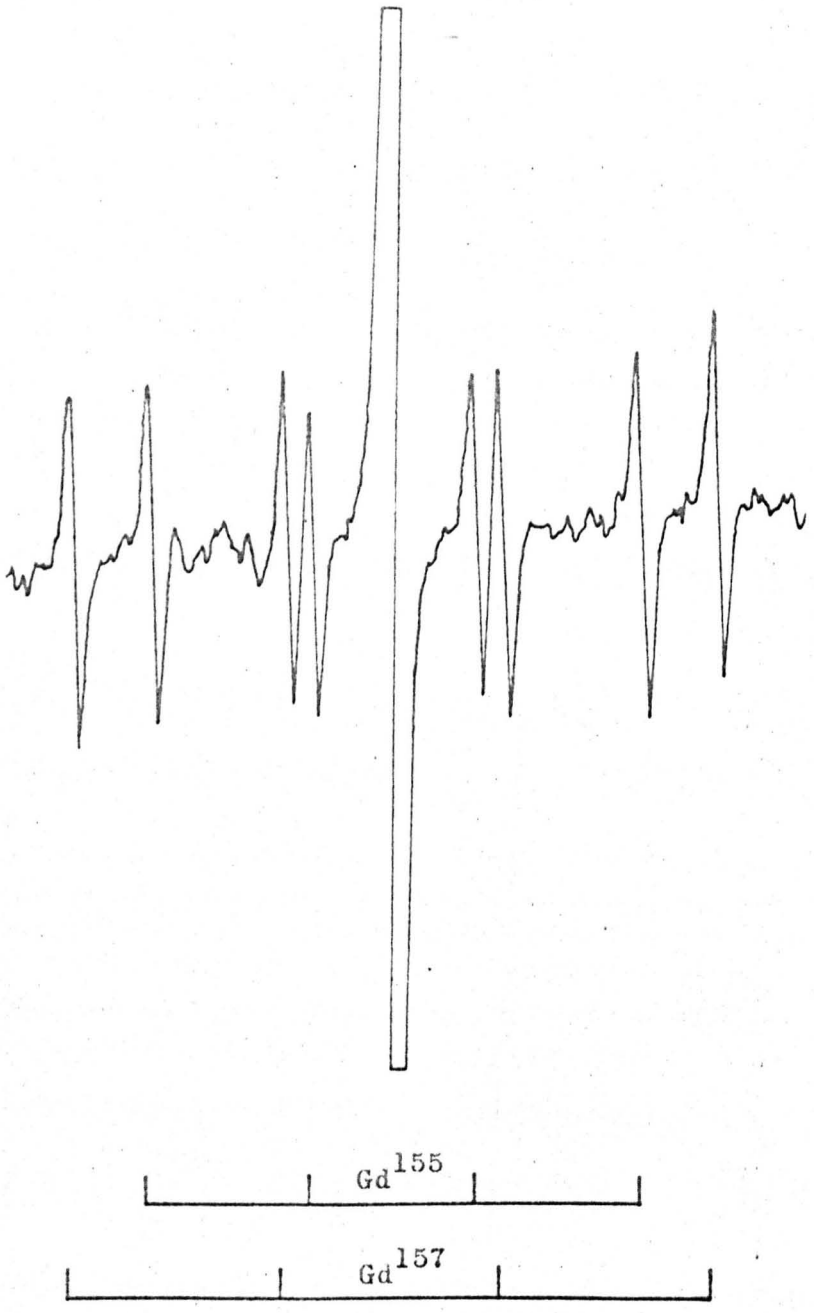

Figure 7.2 Gadolinium hyperfine structure on the $M_s = \frac{1}{2} \leftrightarrow -\frac{1}{2}$ transition of the Gd^{3+} spectrum at 77°K.

consistent with (39) and (40). No forbidden $\Delta M_S = \pm 1$, $\Delta M_I = \pm 1$ transitions were observed away from the principal axis as were seen for Eu^{2+} in calcium oxide (40). Nor were any spectra observed exhibiting axial symmetry, due for example to local charge compensations. It is concluded that the large majority of Gd^{3+} ions are charge compensated remotely, as is also found for Fe^{3+} and Cr^{3+} in calcium oxide.

Two isotopes of gadolinium have non-zero nuclear moments. They are the 14.68% abundant Gd^{155} and the 15.64% abundant Gd^{157} each with nuclear spin = $3/2$. Therefore for the above transitions one expects two groups of four lines centred on each fine structure transition since the hyperfine splitting is generally much smaller than the cubic field splitting. These lines will be about 0.06 of the intensity of the central line due to the even isotopes for each of the fine structure transitions. The spectrum obtained for the $M_s = \frac{1}{2} \leftrightarrow -\frac{1}{2}$ transition is shown in Figure 7.2, and the hyperfine parameters are shown in table 7.2 below.

Table 7.2

Hyperfine Constants for Gd^{3+} in Calcium Oxide

Temperature	A^{155}	A^{157}	A^{155}/A^{157}
290°, 77°K	3.60	4.70	0.767
	±0.1	±0.1	

A is given in units of $10^{-4}cm^{-1}$.

The term A is proportional to the nuclear moment divided by the spin: $\mu/I = g_N$, and the overlap of the magnetic electrons on the nucleus. Since the f electron wavefunctions have negligible expectation at the nucleus, the interaction is thought to arise from configuration interaction involving S electron wave functions. In the case of gadolinium the ratio of the A parameters for the two isotopes is different from the ratio of the nuclear g value. This difference is known as the hyperfine anomaly which is expressed by:

$$\frac{A^{155}}{A^{157}} = \frac{g_N{}^{155}}{g_N{}^{157}} (1 + \Delta) \qquad 7.2d$$

Since the ration $g_N{}^{155}/g_N{}^{157}$ is known to be 0.80 (43), it can be seen that Δ is of the order of 4%. The hyperfine anomaly is thought to arise from a non uniform distribution of unpaired electron spin density over the magnetically structured nucleus (44) which is evidently different for the two isotopes. Similar results have been observed in Gd^{3+} hyperfine structure in other environments both where the symmetry is cubic and lower than cubic (45,46).

7.3 Ti^+

(a) Transiently stable spectrum

The discovery of a spectrum that has been attributed to the $3d^3$ ion Ti^+ in octahedral sites occurred as a result of a search for an excited state spectrum of the F centre. As has been mentioned in section 7.1, the ground state of this centre is a ^1S_o level which is diamagnetic.

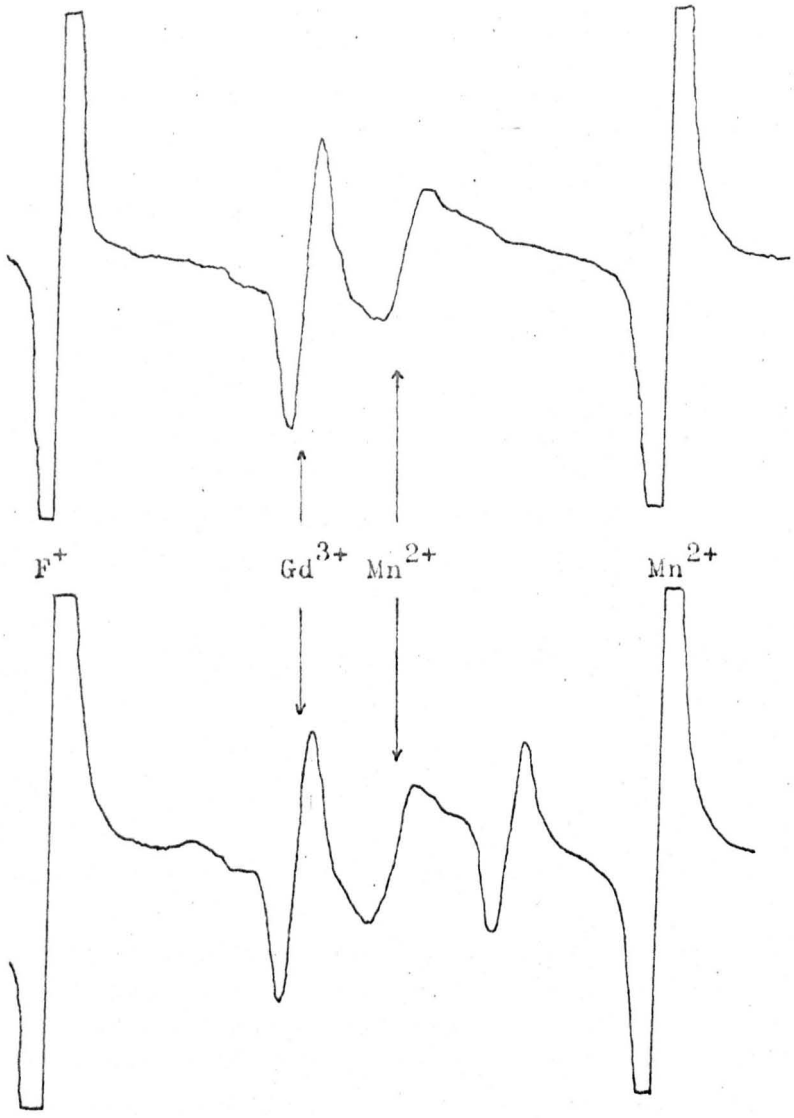

Figure 7.3a Photoexited spectrum at room temperature. Top without, and bottom with ultraviolet radiation. Other lines arise from defects as labelled. Note increace in intensity of F^+ spectrum during irradiation shown by increaced width.

However in the coloured crystals it was observed that a long lived red fluorescence occurred as a result of exposure to ultra violet light from a high pressure mercury lamp. The fluorescence was sufficiently long lived, with a half life of tens of seconds at both room temperature and 77°K, that it was thought possible that it may be due to a forbidden transition between a triplet and a singlet level. This is only weakly allowed and hence the excited state is very long lived, Preliminary investigations using optical filters indicated that the fluorescence was most strongly excited by radiation in the very near ultra violet, possibly therefore in the 3.1eV band of the F centre. Subsequent experiments using a monochromator confirmed that it was in fact either in this band or one very near it that the excitation was occurring. It seemed plausible that a triplet state of the F centre was being excited and, as a result of the long lifetime E.S.R. may be detected for this state. Using the rectangular H_{012} cavity with radiation slots cut in it, spectra were taken first without the radiation and then with it. The results obtained are shown in Figure 7.3a, which were obtained at room temperature. The line seen during irradiation was isotropic with a g value of 1.9866. Observing the spectrum on the oscilloscope revealed that it decayed with a characteristic time similar to that of the fluorescence, although precise measurements could not easily be made.

It was thus assumed that this resonance was due to an excited triplet state of the F centre, that was being populated by some radiationless transition. The excited levels of the helium atom are in order of

increasing energy ^3S, ^1S, ^3P and ^1P. While it is not known whether precisely the same ordering occurs for the F centre, the absorption band at 3.1eV is most probably due to excitation from the ground state to the ^1P level (8). It is possible that radiationless transitions could occur to either the ^3S or ^3P state and while it was not clear which level was responsible, the ^3S was favoured. The reasons were the following: firstly, the single isotropic line, with derivative peak to peak width one gauss, indicated that there was no zero field splitting (larger than the linewidth). This in turn implied accurately cubic symmetry of the defect. The ^3S state is an orbital singlet and thus the symmetry of the defect would be unaltered, but the ^3P is a triply degenerate orbital level and the Jahn-Teller effect would be expected to distort the complex to leave one of the levels lowest; the result would be an anisotopic spectrum or if the effect were dynamic at room temperature, a broad line. Since neither were observed it was initially concluded that the level was ^3S.

However certain anomalous behaviour of the resonance at lower temperatures, intermediate between room temperature and 77°K, and the observation of a stable spectrum produced by radiation at 77°K dictated a more thorough investigation of the temperature dependence of the transient spectrum.

The spectrum produced at 77°K by ultra violet irradiation, had a g value of 1.9866 also, although it was at first thought to be the same as that of Gd^{3+} with g = 1.9925. In fact the central line of this spectrum,

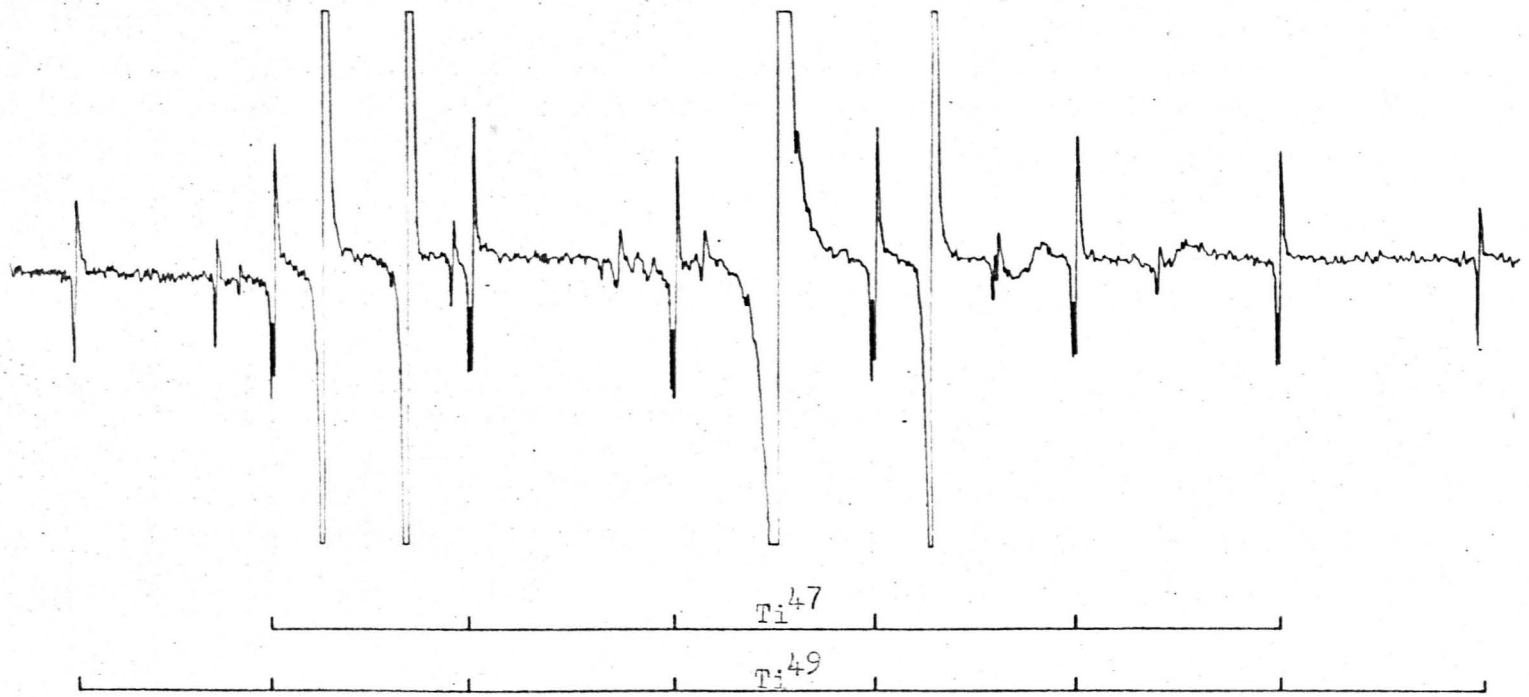

Figure 7.3b. Ti^{+} spectrum at $77^{o}K$. The central line arises from even isotopes. The hyperfine structure from the isotopes Ti^{47} and Ti^{49} is clearly resolved, and an isotopic g shift can be seen between their spectra. Unlabelled lines arise from other defects.

thought to be coincident with the $M_s = \frac{1}{2} - -\frac{1}{2}$ transition of Gd^{3+} showed an orientation dependant broadening at 77°K which at the time was attributed to the partial splitting of these two spectra as a result of a second order dependance of this Gd^{3+} transition on the fine structure splitting.

(b) Hyperfine structure of the spectrum, assignment to $3d^3$ ion

However the vital clue to the origin of this spectrum lay in the hyperfine structure associated with the defect which is shown in Figure 7.3b. An examination of a table of nuclear isotopes revealed only one possible element as a candidate for this defect, which had two nuclear isotopes of fairly low abundance with similar nuclear moments and nuclear spins I of $5/2$ and $7/2$, the majority of the element having I = 0. The element is titanium of which Ti^{47} is 7.75% abundant and Ti^{49} is 5.51% abundant. The remaining isotopes are even and give a single line at the centre of the spectrum. It is found that the spectrum can be fitted to the Spin Hamiltonian:

$$H_s = g\beta \underline{H}.\underline{S} + A\underline{I}.\underline{S} \qquad 7.3a$$

where the spin $S = 3/2$ and I takes the values mentioned above. The energy levels in a magnetic field given by a solution of 7.3a are:

$$E = g\beta HM + AM_m + \frac{A^2}{2g\beta H}\{I(I+1)M - S(S+1)m + Mm(M-m)\} \qquad 7.3b$$

where M and m are the electron and nuclear magnetic levels respectively.

The solution is not exact and higher terms in A give finite but negligible contributions and may therefore be neglected. The resonance fields H, for constant microwave frequency ν are given by:

$$H = \frac{h\nu}{g\beta} - \frac{Am}{g\beta} - \frac{A^2}{2g^2\beta^2 H_o}\{I(I+1) + m(2M-m-1)\} \qquad 7.3c$$

where H_o satisfies $h\nu = g\beta H_o$. The experimentally determined parameters are $g = 1.9866$ and $A^{47} = A^{49} = 10.8 \pm 0.1 \times 10^{-4}cm^{-1}$. It can be seen from Figure 7.3b that there is an isotopic g shift between the spectra from Ti^{47} nuclei and Ti^{49} nuclei, which is about 0.00008. Unfortunately uncertainties in the magnetic field prevented the experimental determination of the direction of shift.

It is in order here to consider carefully how this assignment has been made, because as far as the author is aware this is the first occasion on which monovalent titanium has been reported as a defect in a solid, and the species is chemically unstable. In the stable oxide TiO_2, rutile, titanium is tetravalent and as such has the closed shell argon configuration, which is isoelectronic with Ca^{2+} and is diamagnetic. At first sight this may be a favourite for the stable state of titanium substituting for calcium, but consideration of its twofold charge excess and small ionic radius of 0.68Å makes it unlikely that it is stable in calcium oxide. It has been suggested (47) that the stable state for titanium substituting for Mg^{2+} in magnesium oxide is Ti^{4+}, but in this case the radii are much more nearly the same (Mg^{2+} : 0.65Å, Ca^{2+} : 0.99Å).

This ion may be reduced by X irradiation to Ti^{3+} leaving axial symmetry in MgO. The ion Ti^{3+} has a single 3d electron and as such invariable undergoes a Jahn-Teller distortion in octahedral sites to leave a singlet ground state. The observation of a high degree of isotropy and the ionic radius of 0.76Å allows a safe disposal of this possibility, and it may be remembered here that this spectrum only occurs in the reduced samples, prolonged irradiation under identical conditions does not produce this spectrum in the colourless crystals, nor crystals annealed in air. Thus ions with a large positive charge can effectively be discounted. It is thought probable that Ti^{2+} is the stable state at room temperature in these reduced crystals, but as this is a $3d^2$ system, no resonance may be observed, as appears to be the case for V^{3+}. Repeating arguments put forward before, $3d^2$ ions have a triplet ground state with the $M_s = 0$ level separated from the $M_s = \pm 1$ levels by a zero field splitting. It seems likely that this is too large to obtain resonance for transitions with $\Delta M_s = \pm 1$ at X band. Ti^{2+} has been reported in calcium fluoride (48), in crystals grown under conditions which favoured vanadium in the state V^{2+} rather than V^{3+}, i.e. reducing conditions. It seems likely that the stable state of titanium in "neutrally" grown calcium oxide may be Ti^{3+}, but Ti^{2+} may be stabilized in reduced crystals. The resonance of Ti^{2+} was detected in calcium fluoride by contrast with calcium oxide, because the substitutional cation site is subjected to eightfold cubic coordination by fluorine ions and the crystal field levels are reversed, leaving an orbital singlet lowest with S = 1. The magnetic sublevels are unsplit

by the cubic field. Under ionizing radiation, electrons are ejected from various centres, as can be determined by the appearance of Fe^{3+} and Cr^{3+} in these crystals after irradiation and trapped at Ti^{2+} (ionic radius 0.90Å) to form Ti^{+} (ionic radius 0.96Å). The author believes that neutral or negatively charge titanium are sufficiently unstable that they may be neglected as possibilities.

Further support for the idea that the ion is a $3d^3$ system comes from the fact that the E.S.R. behaves very similarly to the other $3d^3$ ions present in these crystals, V^{2+} and Cr^{3+}; the linewidths are similar (Table 7.1). In an attempt to resolve splitting of the outermost pair of lines due to a second order dependence of the three transitions for an $S = 3/2$ system when $I \neq 0$ (12) as predicted by equation 7.3c, experiments were made at $4^{\circ}K$. All paramagnetic species were saturated beyond detection at this temperature, at the lowest powers available. It is probable that spin lattice relaxation has ceased being a broadening mechanism at $77^{\circ}K$ and no further linewidth reduction would have been observed on lowering the temperature. It was estimated that the maximum splitting obtainable from this second order effect was about 0.1gauss, and thus scarcely resolvable unless further linewidth reduction occurred. Furthermore the $\pm\frac{1}{2} \leftrightarrow \pm\frac{3}{2}$ transitions were probably broadened by lattice defects anyway (12) as was observed for V^{2+} in these crystals, and thus broadened almost beyond detection for low intensity spectra.

The g values of $3d^3$ ions which have been observed in calcium oxide may be listed:

Ti^{+}	:	1.9866	This thesis
V^{2+}	:	1.9683	(11)
Cr^{3+}	:	1.9732	(11)
Mn^{4+}	:	1.9931	(11)

It would be expected that they would form a continuous series, and the departure of the trend by the titanium g value may be considered as grounds for doubting the assignment to Ti^{+}. For $3d^3$ ions in octahedral symmetry the departure from the free spin g value due to spin orbit coupling to the first excited orbital level is given (49) by

$$g = 2.0023 - \frac{8\lambda'}{\Delta} \qquad 7.3b$$

where g is the $3d^3$ ion g value, λ' is the spin orbit coupling constant of the ion in the complex, and $\Delta = 10Dq$ is the splitting of the ground level $^4A_{2g}$ from the $^4T_{2g}$ primarily as a result of the electrostatic effect of the ligand ion (see Figure 2.2). One would generally expect, and does find where measurements are available, that the parameter Δ would increase with charge as a result of the overall attraction of the magnetic $3d^3$ ion for the six ligand ions. If a purely ionic model is taken $\lambda' = \lambda_o$ which is the free ion spin-orbit coupling constant for the ground term, being positive for $3d^3$ ions. Unfortunately owing to covalency effects the ionic complex value of λ' is not the same as the free ion

value, and furthermore the ratio λ'/λ_o is not constant for different ions with the same configuration. Thus it is argued that the breaking of the series by this g value is not grounds for considering the ion other than $3d^3$. The isotropic g value, similar spin lattice relaxation to other $3d^3$ ions, similar ionic radius to Ca^{2+} and the circumstantial evidence of chemical reduction in these crystals, point strongly to a $3d^3$ configuration. The isotropic hyperfine interaction indicates that it arises from the paramagnetic defect itself, rather than from a transferred hyperfine process. The off-axis broadening of the lines is consistent with nearby lattice defects broadening the $\pm\frac{1}{2} \leftrightarrow \pm\frac{3}{2}$ transitions.

(c) Electron trapping to form Ti^+

It is now apparent that the ion Ti^+ is transiently stable when formedby irradiation at room temperature. The spectrum under irradiation was at least a factor of 10^2 more intense than without irradiation at room temperature. As the temperature was lowered using the nitrogen gas flow system, it was observed that the integrated intensity of the spectrum increased, as well as the linewidths reducing, but the ratio of intensities with and without irradiation became smaller. This indicated that the electron trapping was more than transiently stable in an increasing proportion of centres as may be expected. In one sample at 145^oK, a transition occurred in which the spectral intensity was the same with or without irradiation. At lower temperature the spectrum was more intense without radiation. At 77^oK the intensity was down by a factor of two during irradiation, and took between 10 and 100 secs to recover full

intensity. If a sample previously not irradiated was irradiated at 77°K the Ti^+ spectrum intensity would increase with irradiation time for up to two or three hours, then appeared to saturate, or grow very slowly. Upon warming to room temperature, the intensity of the spectrum decayed only slowly, the decay being only noticeable after a few hours, and with a half life of the order of a day. Reirradiation for only a few minutes would restore the original strength. Evidently the history of irradiation was important and precisely quantitatively reproducible results were difficult to obtain.

The distribution, and redistribution under irradiation of the "excess" electrons in these crystals is clearly a complex process involving many centres, some of which may not be detected by paramagnetic experiments in any of their states. It is not possible to explain even qualitatively all the observations made without more experimental data obtained under controlled conditions. These would include handling of crystals under photographic darkroom conditions for periods of many weeks, as it is evident that red light can influence the distribution of electrons (8) in CaO:Ca and that the relaxation times to equilibrium states of distribution are many days in some cases at room temperature, and probably indefinite at 77°K. However, it is worth putting forward a few tentative ideas which may offer some sort of explanation.

In view of the apparent difference in stability of spectra depending on irradiation temperature, it seems probable that the source of electrons may be substantially temperature dependent. At 77°K the

predominant differences observed in the E.S.R. spectrum after prolonged irradiation were the appearance of Fe^{3+}, Cr^{3+} and hole centre spectra in that order of intensity. These are certainly as a result of ejection of electrons. The changes were about as stable as the Ti^{+} spectrum. A small transient increase in the F^{+} centre spectrum was observed, which quickly decayed upon removal of irradiation, as reported in (8). This is attributed to cross bleaching between F and F^{+} centres. Some electrons excited by 3.1eV radiation in the F centre are ionized leaving an F^{+} centre. The free electron presumably is transiently trapped elsewhere. In view of the small integrated F^{+} centre density, the small increase under radiation, and the transient nature of electron release, this is not thought to be a dominant source of electrons for the conversion $Ti^{2+} \rightarrow Ti^{+}$ at this temperature. It was noted that the Ti^{+} spectrum was reduced in intensity under irradiation at $77^{o}K$. This may be due to a transient hole trapping process, but since the spectrum is formed stably under these conditions, a more likely process seems that some of the Ti^{+} centre are being excited into the $^{4}T_{2g}$ state amongst others (see Figure 2.2). While the difficulties of interpreting the optical absorption spectra may make it virtually impossible to measure 10Dq for this ion, because of the large number of other impurities present, it may be possible at least in principle to measure this splitting by irradiating through a monochromator, and noting the radiation energy when the E.S.R. spectrum is most reduced. Using the g value and this energy would enable the bound ion value for the spin orbit coupling constant λ'

to be determined from equation 7.3b. Unfortunately the rather large amounts of energy that would have to be handled by the monochromator and the careful control of incidental light would pose some problems.

None of the centres formed stably at 77°K are so formed at room temperature. Instead the principal source of electrons may be ionization of F centres. Under irradiation the F^+ spectrum became as much as seven times as intense in some crystals, compared with less than one and a half times at 77°K. If this is the correct explanation, then evidently the traps such as Fe^{3+}, Cr^{3+} and V centres must lie intermediate in energy between Ti^+ and the F and F^+ centres. Ti^+ most probably lies near the conduction band, and is easily thermally ionized. The F and F^+ centres are evidently well below the conduction band. When Ti^+ is ionized at room temperature and the original donor was an ionized F centre, then there is a good chance that this will trap the electron, with little chance of thermal re-ionization. If on the other hand Fe^{3+} was the donor then it may provide a weaker trap for the electron, resulting in lower probability of electron trapping. The electron then has a relatively larger chance of being retrapped by Ti^{2+} to form Ti^+.

7.4 F^+ Centre

Generally, heavy particle irradiation is required to produce anion vacancies in the alkaline earth oxides. Ionizing radiation (photons) cannot, even in the γ ray region of the spectrum, transfer sufficient momentum to the anions to produce displacement. In addition extensive

grinding of powders can produce these displacements presumably by the movement of dislocations through the crystallites. Finally they may be produced by heat treatment in metal vapour, but not in vacuum. As has been discussed earlier, some of the crystals used in the present work had suffered this last process accidentally in the growth process. The mechanical processes, i.e. the first two, produce predominantly F^+ centres. The electrons are trapped without further treatment, and thus ionizing radiation does not enhance, or weaken spectra due to F^+ centres (but compare with V centres, section 7.5). In the heat treated crystals both F^+ and F centres are formed and the actual distribution is sample, and sample history dependent. In one sample it was found that the F^+ spectrum could be made seven times as intense, transiently, by irradiating at room temperature with the unfiltered output of a 250Watt mercury vapour lamp through slots in the E.S.R. cavity. In spite of rather low overall concentrations of F^+ centres, the very small linewidth of less than 0.02 gauss, suggested that it may be possible to detect the transferred hyperfine structure due to the overlap of the electron on the neighbouring ions.

Of the naturally occurring isotopes of calcium and oxygen only Ca^{43} which is 0.13% abundant with $I = 7/2$ and O^{17}, 0.037% abundant with $I = 5/2$ are magnetic, and will thus produce a nuclear hyperfine splitting of the F^+ centre E.S.R. line. The anion vacancy has six nearest neighbour calcium ions. For an arbitrary direction of magnetic field pairs of these ions will be equivalent, because the centre has inversion symmetry, and

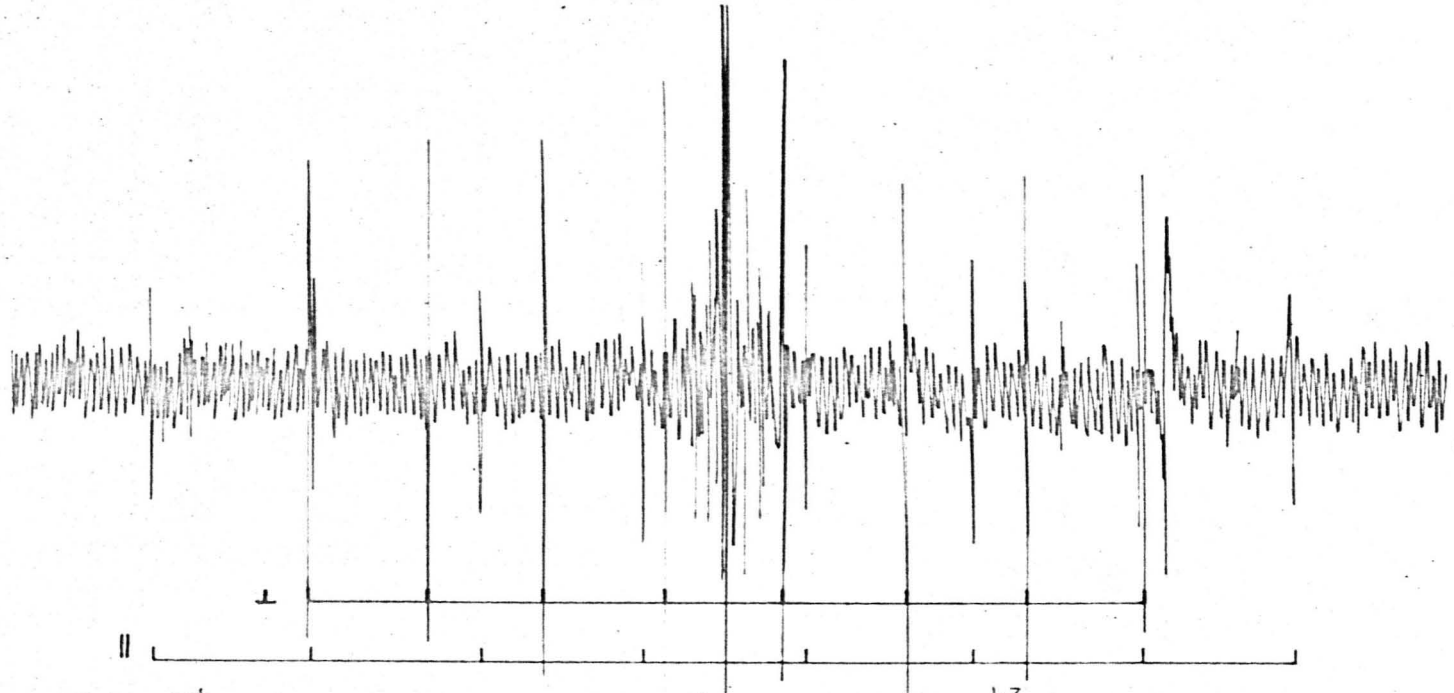

Figure 7.4a. F^+ spectrum showing hyperfine structure due to Ca^{43} nuclei on nearest neighbour sites. The noise components on the original chart extended to higher frequencies.

since I = $^7/_2$ each pair will give a set 8 lines which are 0.03% the intensity of the main line for which there is no splitting by nearby nuclear isotopes. The probability of there being two or more Ca^{43} ions in nearest neighbour positions is clearly very low and may be neglected. Measurements in powders enriched with Ca^{43} (7) suggested that the spectrum would extend over about 100 gauss. Clearly the signal to noise ratio would ultimately determine the feasibility of the experiment, but a problem arose here in that one expected the hyperfine components to have a similar linewidth to the main line (20 milligauss) and for the field to sweep through a resonance in a time greater than the time constant, the sweep rate must be slower than $20mg/\tau$ where τ is the integrating time constant on the output of the phase sensitive detector. Taking the condition that the spectrometer swept 100 gauss in 100 minutes suggests that only 0.5sec time constant could be used. This is rather prohibitive as the normal way of enhancing weak spectra is to use long time constants, e.g. 10 secs. The use of a computer of average transients was not considered feasible in this case as the field sweeps required would be prohibitively difficult to reproduce. However, using ultraviolet irradiation continuously to enhance the spectra, the spectrum shown in Figure 7.4a was obtained at room temperature in the <100> direction, with 100 gauss sweep in 100 minutes using a time constant of 1 sec obtained by double section filtering, which allows a fast rise time, and hence minimum distortion of line. For this case two of the pairs of positions for the Ca^{43} nucleus are equivalent, and perpendicular to the field, and the other pair are parallel.

The spectrum may be summarised following (50) by the spin Hamiltonian:

$$H_s = g\beta \underline{H}.\underline{S} + a\underline{I}.\underline{S} + b(3I_z S_Z - \underline{I}.\underline{S}) \qquad 7.4a$$

where the first term is the usual electron Zeeman term and the second two are an expansion of the term $\sum_n \underline{S}.\underline{\underline{A}}_n.\underline{I}_n$ in equation 3.5. for the transferred hyperfine interaction, in this case with only one nucleus. For a weak axially symmetric hyperfine interaction with one nucleus (i.e. a, b << gβH) the $\Delta M_s = \pm 1$ transitions are given by:

$$h\nu = g\beta H \pm M_I\{(a-b)^2(1-\cos^2\theta) + (a+2b)^2\cos^2\theta\}^{\frac{1}{2}}$$

$$\simeq g\beta H \pm M_I\{ a + b(3\cos^2\theta - 1)\} \qquad 7.4b$$

where θ is the angle between the field direction and the crystal direction joining the nucleus to the defect centre. The parameters a and b clearly represent an isotropic and an anisotropic component of the hyperfine interaction. The isotropic component arises from partial occupation of the ligand s electron wave function by the F^+ centre electron, and the anisotropic component arises from the dipolar interaction between the electron magnetic moment and the nuclear magnetic moment. Angular rotation studies showed that the transitions fitted 7.4b, with g = 2.0000 ± 0.0005, a = 9.17 ± 0.1 gauss and b = 0.97 ± 0.1 gauss. The resonance lines of the hyperfine spectrum show a g shift given by the formula (70):

$$g_{corr} = g\{1 - \tfrac{1}{2}(\frac{a}{H_o})^2(I(I+1) - M_I^2)\} \qquad 7.4c$$

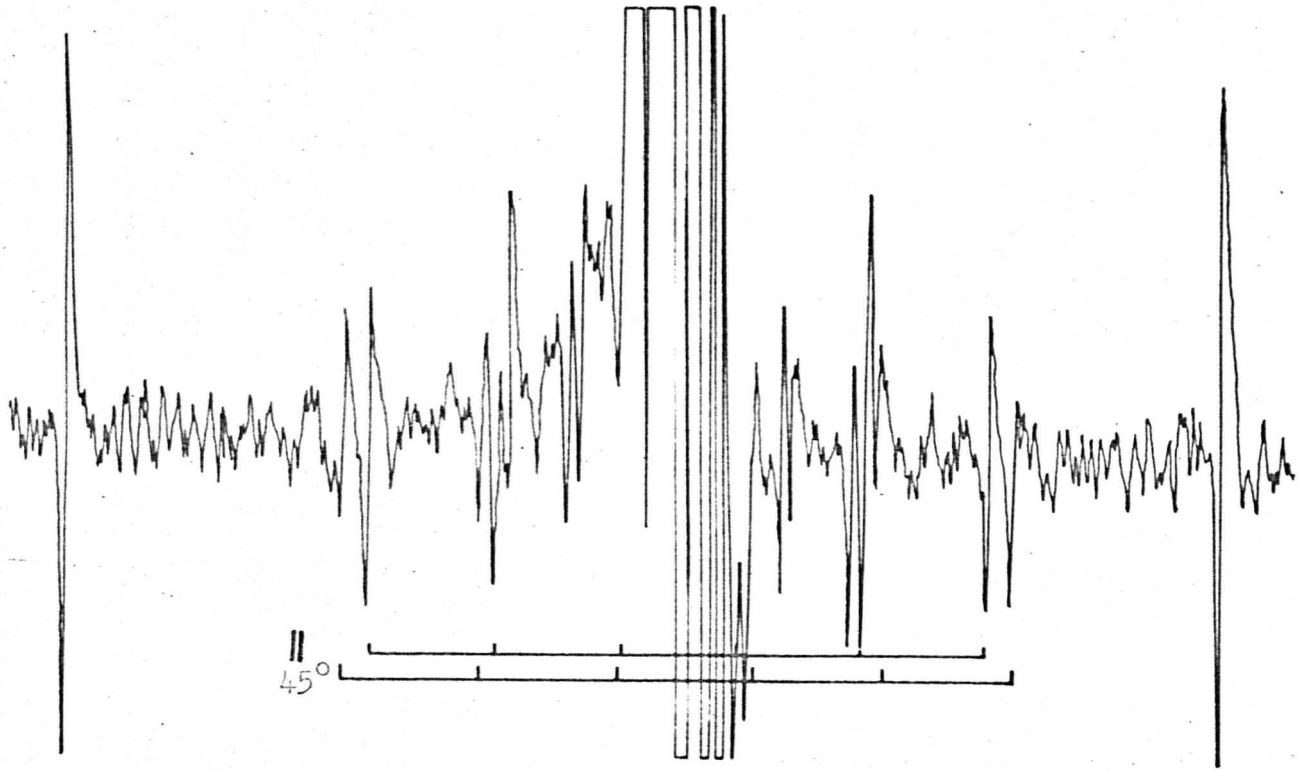

Figure 7.4b. F^+ spectrum within inner pair of assigned lines of Fig.7.4a. Assignments are tentatively made for || and 45° components of O^{17} hyperfine structure. Further splitting of the central line is mainly due to modulation sidebands.

The two inner lines of the spectrum showed a g shift of (g_{corr} - g) of -0.00015 ± 0.00005 which is in good agreement with the predicted value from 7.4c of 0.00015. The anisotropic contribution has been neglected as it is insignificant in this case.

Close examination of the region between the inner pair of lines in Figure 7.4a reveals further weaker lines, and Figure 7.4b shows this part of the spectrum also in the crystallographic 100 direction with a 10 gauss sweep in 100 minutes and a time constant of 10 seconds. An attempt has been made to fit this spectrum to the Hamiltonian 7.4a for the case where one O^{17} ion is in the next nearest neighbour shell. Since O^{17} has I = $5/2$, one expects groups of six lines. In the <100> direction there are four next nearest neighbour ions in directions perpendicular to the field, and eight at 45° to it. Since the group with the larger splitting appears to be weaker it is assumed it arises from the perpendicular ions and the other group from the eight at 45° to the field. This implies a and b are of opposite sign. O^{17} is 0.037% abundant which means that again considering only the case where one ion is interacting, the intensity of the lines should be 0.012% of the intensity of the main line for each pair. The eight at 45° should produce lines four times this intensity, i.e. 0.05% compared with the predicted intensity of 0.06% for the two inner lines of the Ca^{43} hyperfine spectrum. Some intensity appears to be missing from the O^{17} spectrum. If one assumes that a and b are of the same sign then it is possible to explain the loss of intensity of the 45° components as being a result

of misalignment of the crystal, resulting in partial cancellation of this group as a result of their being in an anisotropic part of the angular rotation compared with the groups at 0° or 90° which are on turning points. Persistent attempts to align the crystal failed to better the intensity ratios however, and it is thought more probable that a and b are of opposite sign. Clearly a good angular rotation of the spectrum would solve this dilemma. One performed at 5° intervals in the {100} plane proved of no avail, as lines could not be reliably followed from one orientation to the next. In the course of another at 2° intervals in the {110} plane a second problem was encountered. Thus the radiation, used continuously in these investigations, has produced additional background spectra which began to dominate the O^{17} spectra. Weak lines, just perceptible in Figure 7.4b had grown into lines comparable in intensity to the others. It is estimated that there were between 100 and 200 lines in this 10 gauss region, all approximately the same linewidth, and therefore presumably due to interactions with the F^{+} centre. The combination of linewidths, line separations and magnetic field uncertainties, all of the same magnitude, combined to make analysis of the angular variation a highly speculative task which has not been completed. None of the radiation produced spectra has been identified with any model. The author is inclined tentatively to assign the spectrum indicated in Figure 7.4b to interaction of the F^{+} centre with one O^{17} nucleus in a next nearest neighbour site. The parameters are $g = 2.0000 \pm 0.0005$, $a = 0.87 \pm 0.1$ gauss, $b = 0.05 \pm 0.02$ gauss and

and a and b are of opposite sign. No g shift was observed for this hyperfine spectrum.

Some calcium oxide crystals were examined that had been neutron irradiated in the Harwell Pluto Reactor to doses of 10^{18} per cc. All of these showed spectra due to the F^+ centre, the latter being dose dependent. The crystals were coloured light green except for the ones with the largest dose which were blue. There was some evidence of line broadening and the linewidth of the F^+ centre spectrum was dose dependent, increasing with increasing dose. The neutron irradiation had partially reduced the crystals to a powder, only a few pieces of single crystal from each sample being sufficiently large for single crystal studies. In some samples many other lines were observed over a 100 gauss range centred on the F^+ centre, but owing to rather low intensities and poor resolution these have not been fully investigated. The symmetry of the defects did not appear to coincide with the crystal symmetry, and it is thought probable that they arose from aggregates of anion vacancies, with trapped electrons. One simple centre was observed which appeared to have axial symmetry along the 100 direction and may be fitted to the spin Hamiltonian:

$$H_s = g_{\parallel} \beta H_z S_z + g_{\perp} \beta (H_x S_x + H_y S_y) \qquad 7.4d$$

where $S = \frac{1}{2}$, $g_{\parallel} = 1.9952$ and $g_{\perp} = 1.9995$. This spectrum showed the usual F centre characteristics of small linewidth at room temperature and rather long spin lattice relaxation time, exhibited by easily

saturable spectra. No satisfactory model has been formulated for this defect. An axial F type centre has been reported in calcium oxide (52), which may be called the F_c^+ centre, which fits the Hamiltonian 7.4c with $g_{\parallel} = 1.9995$ and $g_{\perp} = 1.9980$. The model proposed for this defect was that of an electron trapped in an adjacent anion and cation vacancy pair. For an axial electron containing centre one expects $g_{\parallel} \simeq 2$, $g_{\perp} \simeq 2 - k\lambda/\Delta$ where k is some function of the polarization of the adjacent cations, λ their spin orbit coupling constants and Δ is the (S - P) separation of the Ca^+ ion. Since λ is positive this predicts a negative g shift for $g_{\perp}$ as is observed for the F_c^+ centre. Thus the spectrum observed in the present work is somewhat anomalous if it is indeed an F type centre. Previous workers have found for some d' systems (53,54) that $g_{\perp} < g_{\parallel}$ and it is possible that this centre is similar to the F_c^+ centre, with some difference, such as a trivalent ion, adjacent to the anion vacancy in the axis of the vacancy pair. Thus a possible model for the defect would be a linear chain in the 100 direction consisting of a diamagnetic trivalent ion, an anion vacancy with a trapped electron and a cation vacancy.

7.5 Hole Centres

(a) Models for the centres

Single hole centres or V_l centres have been reported previously in calcium oxide (55,56) following irradiation at $77^{\circ}K$. An analogous centre has been reported in magnesium oxide (10) and the model then proposed was a trivalent ion such as Cr^{3+} in a next nearest neighbour

position along a 100 direction to a vacancy which had trapped a hole. In view of the single axis the defect showed it was assumed that the hole was trapped on an oxygen ion on the opposite side of the vacancy from the trivalention. Increasing linewidths at temperatures above 77°K were assumed due to hopping of the hole around the anions. While the trivalent ion was then assumed to be necessary for charge stability two problems were raised, one of which was explicitly recognized. This was the expectation that for a hole trapped near a magnetic ion there would be some evidence of dipolar interaction which was not observed. The second is that if the hole hopped onto one of the other anions, the defect would exhibit different symmetry and one or two other resonance spectra should have been observed at the higher temperatures at least, resulting in loss of intensity from the simple spectrum as well as broadening. It was not stated whether this occurred or not. In a subsequent publication (51) it was conceded that the trivalent ion was not necessary for the defect's stability and thus the model was simply a hole trapped on an anion adjacent to a cation vacancy. This is the V_1 centre proposed by Seitz (57). The increasing linewidth with temperature was more satisfactorily explained as a jumping of the hole from anion to anion, and the difficulty of saturating the E.S.R. transition at 77°K as due to spin lattice effects within the O^- ion as a result of spin orbit interaction. This may be compared with the F^+ centre which is magnetically well isolated from the lattice.

The resonance spectrum consists of three lines arising from the three equivalent 100 axes, which have equal numbers of defects. The spin Hamiltonian appropriate to such a defect may be written:

$$H_s = g_{||} \beta H_z S_z + g_{\perp} \beta (H_x S_x + H_y S_y) \qquad 7.5a$$

where $S = \frac{1}{2}$. When the field is directed along the principal axis the spectrum becomes two lines with one at $g_{||}$ and the second with twice the intensity at $g_{\perp}$. In addition to these three prominent lines several others were observed in the present work with the same angular variation. They were unresolved at the $g_{||}$ orientation, but showed measurable splittings at $g_{\perp}$. The g values measured for hole centres in calcium oxide are listed in table 7.5 below. The range of $g_{\perp}$ is shown for the additional weaker lines.

Table 7.5

E.S.R. parameters for hole centres in calcium oxide

	$g_{||}$	$g_{\perp}$	D
V_1	2.0028	2.0670	-
	2.0028	2.0680	-
	2.0028	2.0660	-
W	2.0023	2.0683	114 gauss

Earlier workers reported similar but significantly different g values for V_1 centres in calcium oxide. The reasons for the differences are not understood at present as they appear to be outside the limits of experimental error. It is also not understood precisely what differences occur for the defects observed in these crystals with different g values, although it is plausible that they may arise from V centres with additional axial fields due to other nearby charge defects. This idea receives some support from the fact that the intensity of these spectra were strongly sample and sample history dependent.

The other principal hole centre spectrum which has been observed is attributed to the W centre, or two holes located on anions on opposite sides of a cation vacancy. This has not previously been reported in calcium oxide although it has been observed in magnesium oxide (10). The spin Hamiltonian appropriate to this defect is:

$$H_s = g_{\parallel}\beta H_z S_z + g_{\perp}\beta(H_x S_x + H_y S_y) + D(S_z^2 - \tfrac{1}{3}S(S+1) \qquad 7.5b$$

with S = 1. The parameters for this defect are listed in Table 7.5. The spectrum consists of six lines. To a first approximation there is a pair of lines centred on each of the three lines belonging to the V_1 centre. Along the principal axis the splitting is 2D. The pairs of lines obey a $(3\cos^2\theta-1)$ law about the V_1 lines where θ is the angle between the defect axis and the external magnetic field. If the interaction is assumed to be dipolar the separation between the point dipoles is found to be 6.3Å compared with the normal anion anion separation of 4.8Å in calcium oxide. These values may be compared with

5.0Å dipolar separation and 4.2Å anion anion separation in magnesium oxide. It can be seen that the ratio of distances is greater for calcium oxide which is presumed to reflect the greater compressibility than magnesium oxide.

For a p state hole in an axial field, the g tensor is of the form:

$$g_{\parallel} \simeq 2, \quad g_{\perp} \simeq 2 - {}^{2\lambda}/\delta$$

where λ is the spin orbit coupling constant and δ the electronic splitting of the p states of the O^- ion in the crystal field. The spin orbit coupling constant is negative for a p state hole, thus one expects $g_{\perp}$ to be greater than 2 and $g_{\parallel}$ near 2, as is observed.

(b) Production of hole centres

In contrast to the production of F centres in the alkaline earth oxides, which can only be produced by heavy particle irradiation, V_I centres are created in reasonable concentrations by ionizing irradiation. Previous authors have used high energy X or γ radiation and 4.9eV radiation from a low pressure mercury arc. In the present work radiation from a high pressure mercury lamp at 77°K produced detectable concentrations of V_I centres in both the reduced (brown) and colourless samples; thus it was possible to have both F and V_I centres present in the same crystal. However, if an oxidizing anneal preceded the low temperature irradiation, considerable enhancement of the V centre spectrum occurred. Generally any F centres present were destroyed by the anneal, but a short anneal at 1300°C (e.g. 10 minutes) followed by quenching did not destroy all

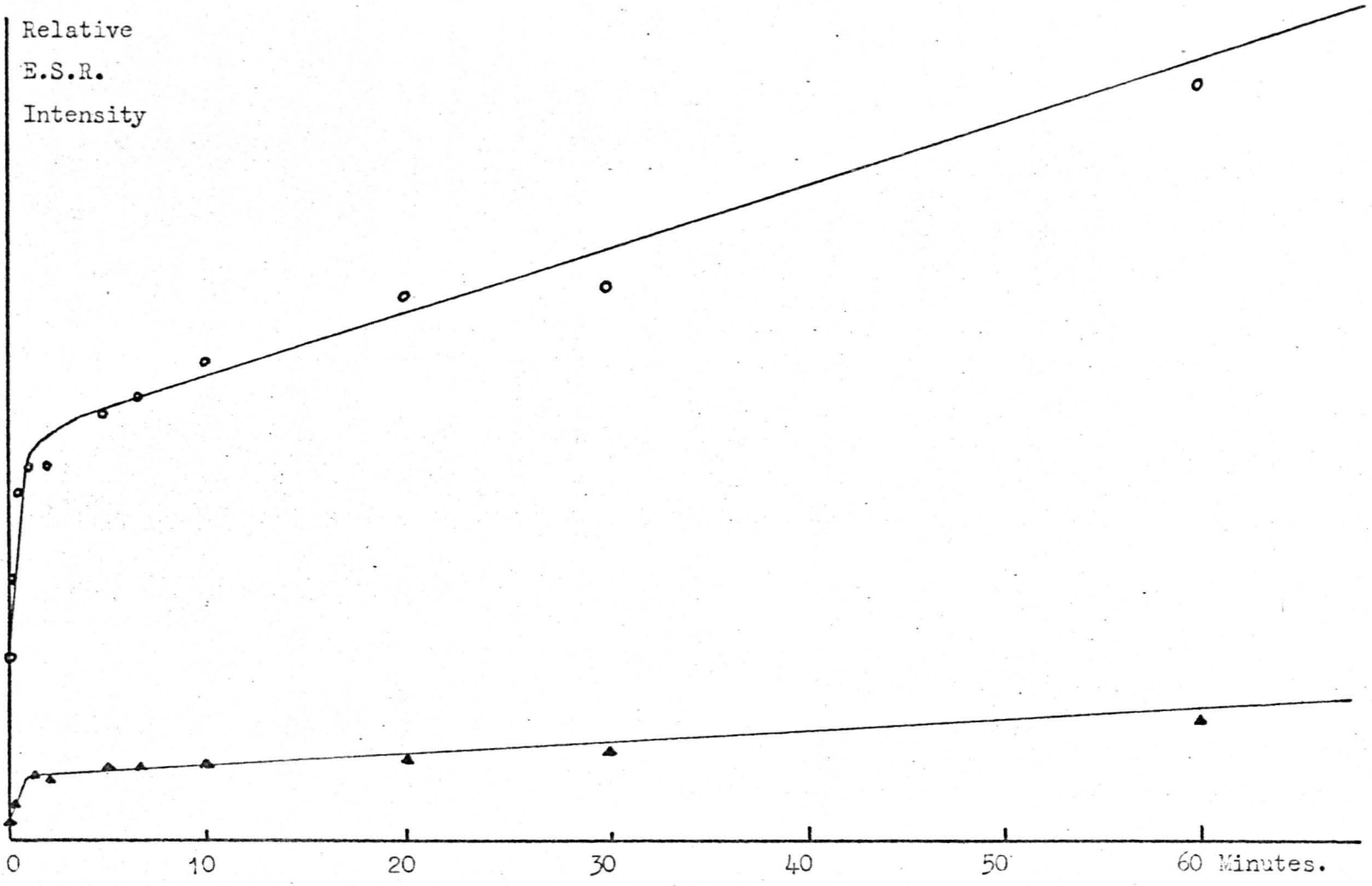

Figure 7.5. Growth of hole centers as a function of ultra violet irradiation dose at 77°K., which is proportional to time. o - V_1 centers ▲ - W centers

F centres in some samples. If samples were quenched after 24 hours or more at 1300°C a small concentration of V centres was found to be present with no irradiation. This is not strictly true as a short period of irradiation by daylight occurred at 77°K, and it has been shown (8) that light of energy less than 2.5eV can have an influence on the state of ionization of defects. However in these crystals this low residual concentration of V centres appeared to be quite stable at room temperature over a period of weeks. If an annealed and quenched crystal was irradiated the V (and W) centre concentration grew to a level dependent on time of irradiation. If the crystal was allowed to warm to room temperature the V centre concentration decayed over a period of several hours or days, depending on the sample, to approximately the original concentration present after quenching. This process could apparently be repeated indefinitely. Figure 7.5 shows how the intensity of V_1 and W centre spectra varied as a function of time of irradiation. The intensity scale is only relative; no attempt was made to estimate the number of photons nor the numbers of centres produced. The relative intensities of V_1 and W centres are proportional to those observed during the experiment. The experimental points strongly suggest that each growth curve may be fitted by a straight line over most of the growth period. In the initial few minutes a high quantum efficiency is found with a rapid growth linear in dose. After this initial period the quantum efficiency falls steeply, but the growth is still linear in dose.

The growth has been followed to higher doses than shown, but no saturation found. Unfortunately no dewar was available for really prolonged irradiation.

The interpretation of the growth curve is not straightforward. There is some evidence that the V centres are themselves occupying a range of energy levels within the band gap or more probably they have, situated at varying distances, defects with variable ionization, which may be occupying a range of energy levels. For the moment it will be assumed that the radiation is merely redistributing electrons within the crystal; no ionic migration is involved. Some of the V centres are stable at room temperature, in contrast to the observations of earlier workers (55,56). This may be due to the known low impurity content of the crystals resulting in some V centres within the oxidized crystals being sufficiently distant from potential donors of electrons that when the donors are thermally ionized, they do in practice generally recapture the electron before it is trapped by the V centre. Another proportion of vacancies lies near a defect that will trap an electron stably at 77^{o}K. These are the V centres formed in the first growth period. The remaining V centres are formed under conditions where there is continual re-ionisation among the defects. This results in a high proportion of V centres formed being destroyed almost immediately, and a consequent slow growth. Unfortunately this explanation does not account for the linear dependence on dose. During both stages of the growth process a logarithmic dependence on dose would be expected as each of the stages

was saturated. It may well be that a sufficiently careful examination of the growth curve would reveal such a dependence. The uncertainties in both irradiation timing and spectrometer gain limited the accuracy in the early region of the curve, thus a logarithmic variation may be found for this process. If one assumes that the radiation is only populating already existing vacancies, then eventually the upper dose region must saturate, as it must in any case of course because the number of possible vacancies in the crystal is limited. One puzzling feature of the strong growth of hole centres is that there is no obvious trap for the considerable number of electrons. During hole centre growth there is also observed considerable growth in Fe^{3+} and Cr^{3+}, presumably from the divalent ions. None of the ions appear to be reduced in the process, except titanium in the reduced crystals. Thus one possibility may be mentioned which is not probable on energetic grounds. The cations may be diffusing to crystal surfaces by vacancy migration inwards, during the second growth stage. The electrons in turn may be being trapped on the cations to form surface metal atoms. If this were occurring one would expect a linear dependence on dose in the range of concentrations observed (not greater than 10^{16}/cc). Furthermore, the idea could be tested because one would expect a thermal threshold below which the vacancy migration could not occur. Thus below some temperature it would be impossible to produce V centres in the second stage of the growth curve.

7.6 Double Quantum Transitions in Mn^{2+} Spectrum

A spectrum has been observed in some of the crystals that have been ultra violet irradiated, or heat treated, or both, that is due to Mn^{2+} ions, but is clearly not part of the normal $^6S_{5/2}$ spectrum in cubic fields. This normal spectrum is present in all single crystals of calcium oxide, and has previously been reported (60). The spectrum has been fitted to a spin Hamiltonian:

$$H_s = g\beta \underline{H}.\underline{S} + \frac{1}{6}a\{S_x^4 + S_y^4 + S_z^4 - \frac{1}{5}S(S+1)(3S^2-1)\} + A\underline{S}.\underline{I} \qquad 7.6a$$

where $S = 5/2$. The first term is the usual Zeeman term. The second term is due to the removal of the degeneracy of the zero magnetic field levels by the cubic crystal electric field and the last term arises from the further splitting of these levels by the nuclear spin $I = 5/2$ in the 100% abundant isotope Mn^{55}. In this case the nuclear splitting dominates the fine structure term, and the spectrum consists of six groups of five lines. The energy levels arising from the Hamiltonian 7.6a when the first term dominates, have been given by Low (61). Within each pentad the transitions $\Delta M_s = \pm\frac{1}{2} \rightarrow \pm 3/2$ and $\pm 3/2 \rightarrow \pm 5/2$ are symmetrically placed about the $\Delta M_s = \frac{1}{2} \leftrightarrow -\frac{1}{2}$ transition. This latter transition has a much smaller linewidth than the other transitions, whose precise positions depend on second order effects from the hyperfine interaction, and thus vary for each pentad.

The additional spectrum observed in the treated crystals consisted of six doublets, each one centred on one of the manganese

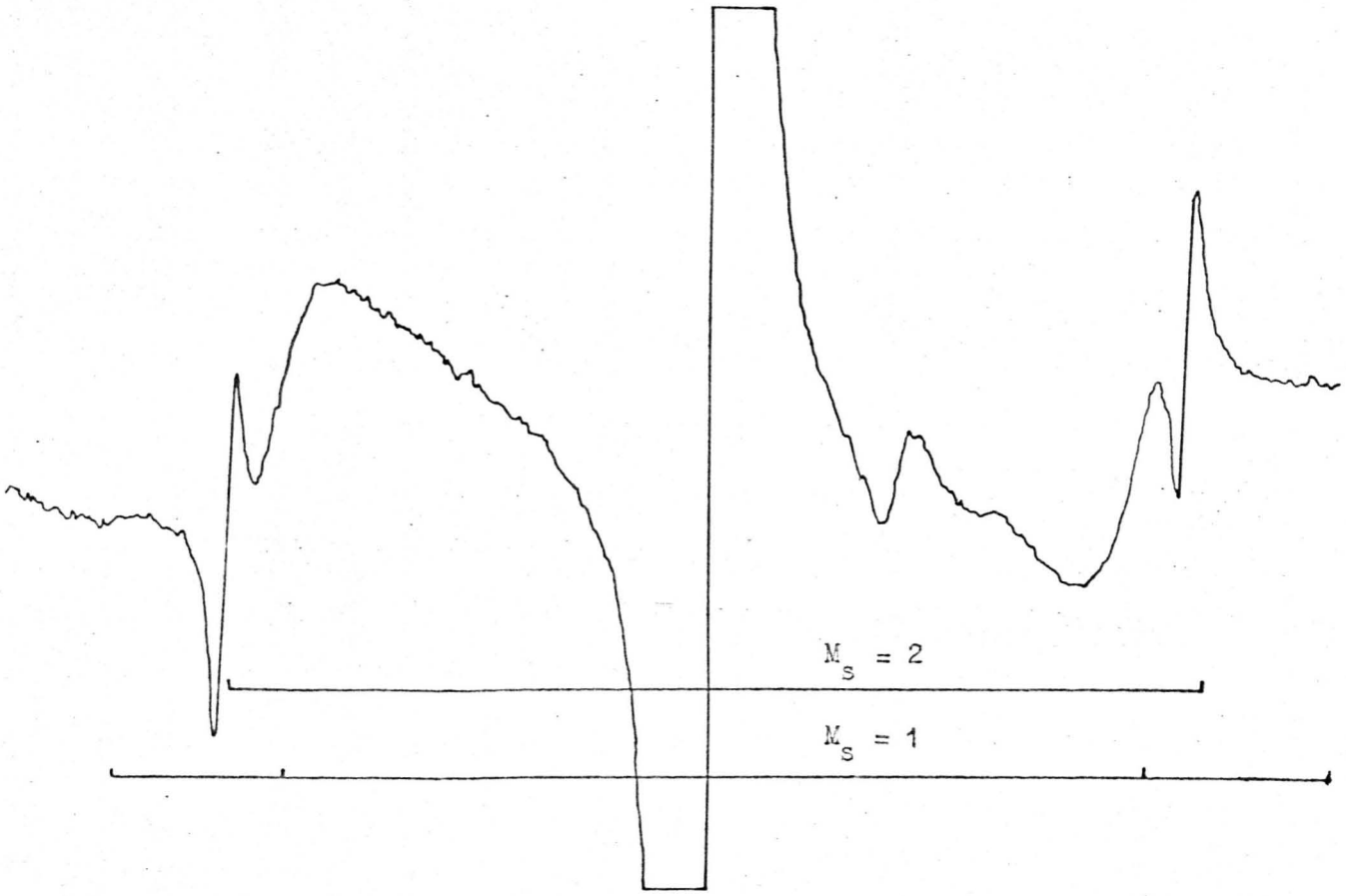

Figure 7.6a. Double quantum transitions in the Mn^{2+} spectrum for $m_I = 3/2$ level.

$\Delta M_s = \frac{1}{2} \leftrightarrow -\frac{1}{2}$ transitions. The linewidths of this spectrum were very similar to the linewidths of the central line of each pentad, and hence although they occurred in positions partially overlapping the fine structure transitions, they could in practice easily be identified. A typical spectrum for one of the pentads is shown in Figure 7.6a. Initially it was thought that this spectrum arose from a centre in which the normal manganese $\Delta M_s = \frac{1}{2} \leftrightarrow -\frac{1}{2}$ transition was split by interaction with a ligand nucleus with spin $I = \frac{1}{2}$. Although in principle one should also observe the other transitions split by this ligand, it was assumed that the lines were not detected because of low intensity and broadening. Thus in writing a Hamiltonian for this defect one may assume an effective spin of $\frac{1}{2}$:

$$H_s = g\beta \underline{H}.\underline{S} + A_1 \underline{I}_1.\underline{S} + A_2 \underline{I}_{2z}.\underline{S}_z + B(S_x \underline{I}_{2x} + \underline{S}_y \underline{I}_{2y}) \qquad 7.6b$$

where A_1 is the isotropic hyperfine parameter for Mn^{55} and takes its usual value of $80.8 \times 10^{-4} cm^{-1}$ in calcium oxide, and A_2 and B are the ligand nucleus transferred hyperfine parameters. The ligand hyperfine energy may then be written as

$$E = a + b(3\cos^2\theta - 1)M_s m_I \qquad 7.6c$$

where $a = \frac{1}{3}(A_2 + 2B)$ and $b = \frac{1}{3}(A_2 - B)$

In this form a is the Fermi contact term:

$$a = \frac{16\pi}{3} \frac{\mu_e \mu_N}{I_N} |\psi_s|^2 \qquad 7.6d$$

and b is the dipolar interaction:

$$b = \frac{2\mu_e\mu_N}{I_N} \langle r^{-3} \rangle \qquad 7.6e$$

where r is the distance between dipoles. Preliminary investigations of the angular dependence of the spectrum indicated that it was highly anisotropic, but a surprising degree of broadening away from the axis made it impossible to follow the spectrum for more than about 25°. Since OH^- groups occur in these crystals frequently it was assumed that the ligand nucleus was a proton and also assuming the interaction to be principally dipolar, as was found for interaction of a V centre with a proton (59), the splitting of 28 gauss for each doublet gave a Mn^{2+} - H separation of 1.46Å. This made the OH bond length, assuming the manganese and oxygen ions were on lattice sites, equal to 0.94Å in good agreement with that bond in calcium hydroxide, 0.936Å (58). Following (59) a search was made for additional infrared bands in the 3000 - 4000cm^{-1} region in the treated crystals, but only a rather weak broad band was observed. Kirklin et al. found sharp bands associated with OH^- radicals trapped near V centres in MgO. More detailed attempts to fit the spectrum to 7.6b revealed that it did not follow a $(3\cos^2\theta-1)$ law, and could not be satisfactorily fitted with any combination of a and b values. Moreover the pronounced broadening offthe axis was not entirely consistent with the proposed model.

Multiple quantum transitions have been observed in magnesium oxide associated with Ni^{2+} (62) and Mn^{2+} and Fe^{3+} (63). The similarity

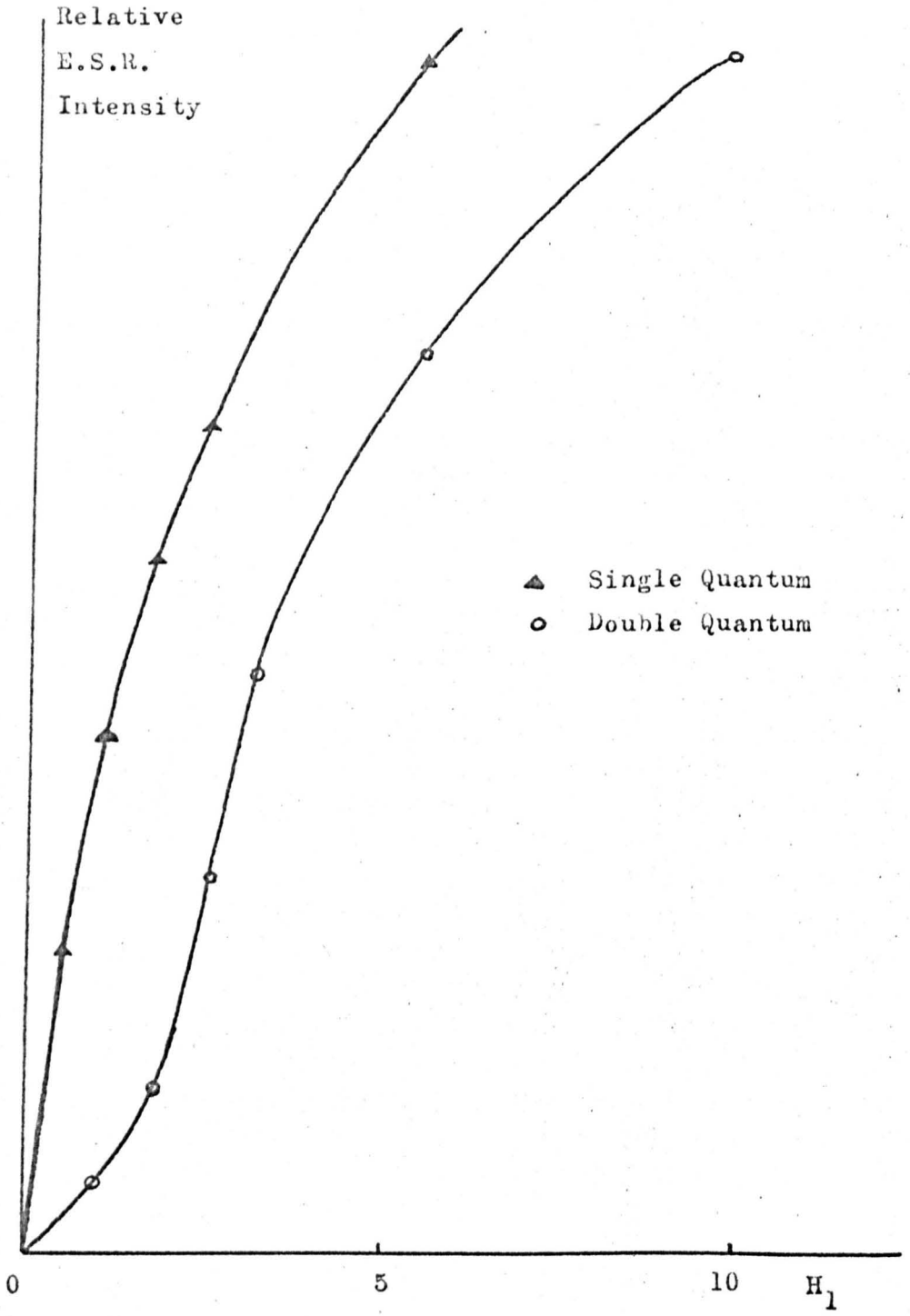

Figure 7.6b. Intensity of ESR signal for single and double quantum transitions in Mn^{2+} spectrum. It can be seen that the double quantum transition intensity rises more than linearly with H_1 before the onset of saturation.

between the present spectrum in calcium oxide and the description of the spectrum for Mn^{2+} in magnesium oxide prompted further investigation of this possibility. One of the characteristics of double quantum transitions is that below the saturation value they increase in intensity more than linearly with H_1, the microwave magnetic field in the cavity. The intensity of the spectrum is plotted in Figure 7.6b against H_1, and for comparison the $\Delta M_s = 3/2 \leftrightarrow \frac{1}{2}$ transition intensity is also plotted. It can be seen that the latter transition is suffering some saturation even at low power levels, whereas the spectrum under investigation at first increases more than linearly, before saturating. This is considered strong evidence in favour of assigning the spectrum to double quantum transitions.
The only absolutely certain test of double quantum transitions, employed by Orton et al. (62) and Auzins and Wertz (63), is to obtain simultaneous absorption of two quanta of different energy. This can be achieved using a bimodal cavity attached to two independent spectrometer systems.

Further support for the idea in the present case comes from the line positions. Neglecting hyperfine and second order terms in a the transition fields for the single quantum lines may be written:

$$
\begin{aligned}
-5/2 \rightarrow -3/2 &: H = (h\nu+2a)/g\beta - 4D \\
-3/2 \rightarrow -\tfrac{1}{2} &: H = (h\nu-5a/2)g\beta - 2D \\
-\tfrac{1}{2} \rightarrow +\tfrac{1}{2} &: H = (h\nu)/g\beta \\
\tfrac{1}{2} \rightarrow 3/2 &: H = (h\nu+5a/2)g\beta + 2D \\
3/2 \rightarrow 5/2 &: H = (h\nu-2a)/g\beta + 4D
\end{aligned}
\qquad 7.6f
$$

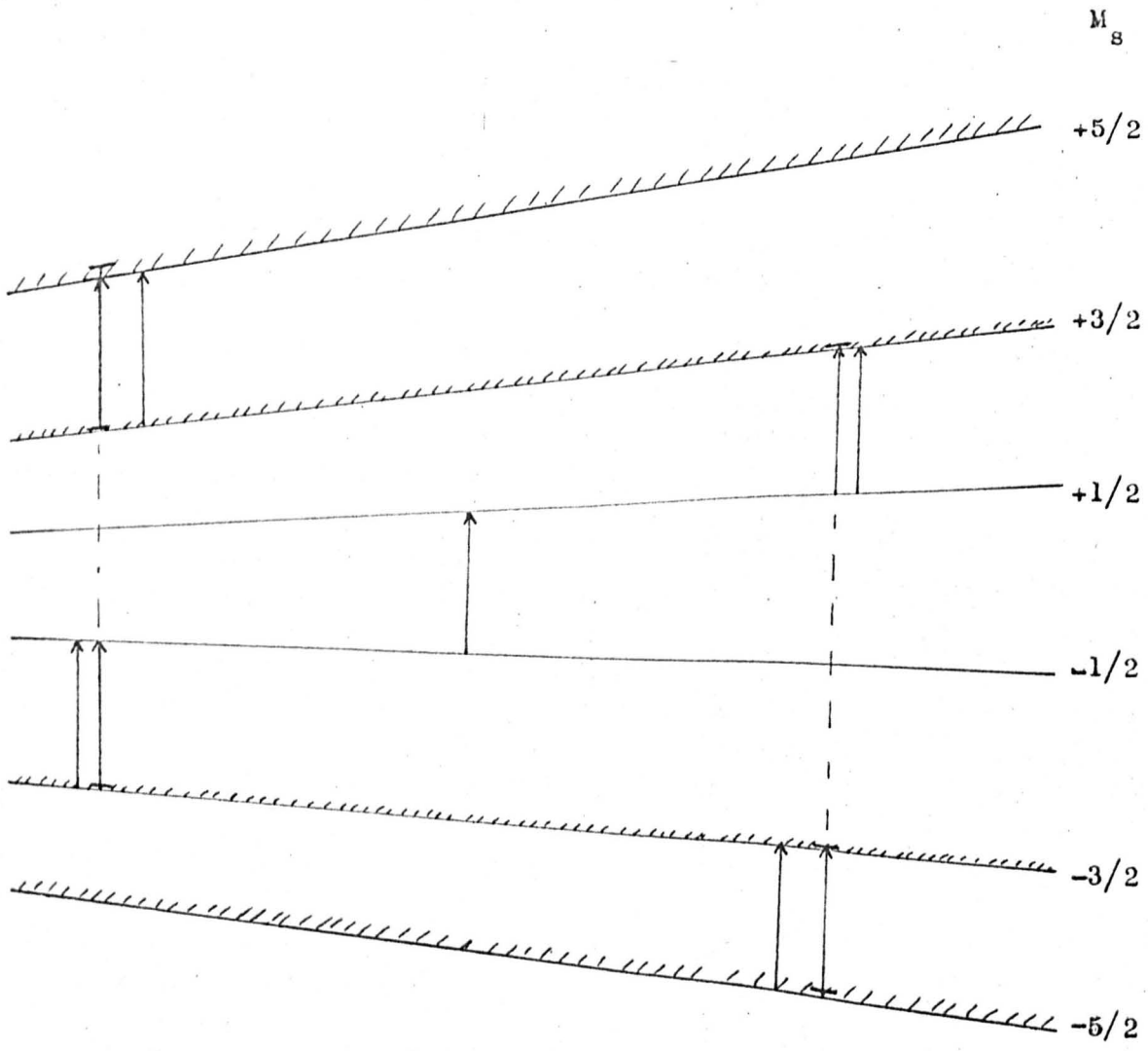

Figure 7.6c. High field energy levels of Mn^{2+} in an octahedral crystal field. The result of a spread in tetragonal distortions of the crystal field, giving rise to a small D term in the spin Hamiltonian, is shown by shading. The $\pm 3/2$ levels are raised 2D, and the $\pm 5/2$ levels raised 6D relative to the $\pm 1/2$ levels. The usual transitions are shown, and also the double quantum transitions between levels coupled by dashed lines.

where the term in D is added to allow for the effect of small tetragonal distortions due to strain and nearby defects. In a study of Fe^{3+} and Mn^{2+} (64) the linewidth of the $\Delta M_s = \pm 3/2 \leftrightarrow \pm 1/2$ and $\pm 5/2 \leftrightarrow \pm 3/2$ lines was found to be consistent with a distribution of D parameters, but inconsistent with a spread in a. In Figure 7.6c the relative effect of a spread in D parameters is shown superimposed on the high field energy levels, neglecting hyperfine interaction. If it is assumed that the D terms leads to equality of the $-3/2 \leftrightarrow -1/2$ and $3/2 \leftrightarrow 5/2$ transitions, one obtains:

$$h\nu - 5a/2 + 2D = h\nu - 2a - 4D \qquad 7.6g$$

which gives D = 0.54 gauss, assuming a = 6.5 gauss (60). If the two transitions occur at the same field then the line must subdivide the field separation of the $-3/2 \leftrightarrow -1/2$ and $3/2 \leftrightarrow 5/2$ such that one third of the separation is between it and the $-3/2 \leftrightarrow -1/2$, and two thirds lie between it and the $3/2 \leftrightarrow 5/2$ transition. Within experimental errors this is found to be true. The intensity of the doublets varied with increasing m value to $m = 1/2$ then decreased. In Figure 7.6a the spectrum for $m = 3/2$ is shown, because the Cr^{3+} spectrum invariably present when this spectrum was seen, partially masked the spectrum for $m = 1/2$. When the field is along the axis the $\pm 3/2 \leftrightarrow 5/2$ transitions lie outside the $\pm 1/2 \leftrightarrow \pm 3/2$ transitions for the $m = 3/2$ transition, due to the hyperfine interaction. Thus the double quantum transitions lie outside the dominant $\pm 1/2 \leftrightarrow \pm 3/2$ fine structure lines. The intensity and temperature variation of this

spectrum may be compared with that for the MgO:Mn system which showed increasing intensity to high field monotonically. In MgO the spectrum was only observed at room temperature, being too weak to observe at 77°K, whereas in CaO it was only observed at 77°K. No mention has been made in the literature of anisotropic linewidths, and thus this aspect of the problem could not be compared.

Since the proposed mechanism for the spectrum to be observed is the existence of lattice distortions it is not surprising that the spectrum is most intense in annealed and quenched samples. It was enhanced by ultra violet irradiation, the action of which must have been to increase the number of Mn^{2+} ions with a D term ≈ 0.5 gauss.

CHAPTER VIII

CONCLUSIONS

Experimental evidence, presented in this thesis has provided information on the way in which defects may be altered in type and concentration in certain ionic crystals by various treatments. Most of the investigations have employed E.S.R. techniques and the most fruitful lines have proved to be heat treatment at high temperatures, as near the melting point as practical, and ultraviolet and visible radiation at lower temperatures, between room temperature and 77^{o}K.

8.1 Silver Halides

It has been shown that the effect of visible radiation in specific temperature ranges on iron doped silver halide crystals may result in not only the more usual redistribution of electrons, but also in ionic displacements in the lattice. In the case of AgCl:Fe the iron is in the form Fe^{2+} at room temperature when in equilibrium. Although spectra from Fe^{3+} have been observed in crystals held at room temperature for some time, they seem to decay eventually, and no instance has been observed of Fe^{3+} spectra appearing after room temperature treatment. Crystals that have been heated in chlorine gas and quenched, show Fe^{3+} spectra, and there is considerable support for the idea that the ion is at an interstitial site tetrahedrally coordinated by four ligand anions, with four ligand cation vacancies. At room temperature or above

depending on the sample, the Fe^{3+} spectrum decays, and some of the Fe^{2+} at least appears to be on cation sites within the lattice, that is not trapped near dislocations. Dislocations may play an important role in the decay process, and there is evidence from the low temperature studies that some iron may be trapped near them. Since the formation of the Fe^{3+} trigonal complex shows a lower limit to the temperature range in which it is formed, 168°K, a characteristic time must exist for the loss of the Ag^{+} ion. It is at this temperature that the competing processes of electron-hole recombination and Fe^{2+}-hole combination balance. The electron lifetime in pure crystals of AgCl is estimated as 10^{-6} or 10^{-7} seconds using previously available data for electron mobility at 170°K in AgCl ($100 cm^2$/volts sec (65)) and assuming an electron range of 10^{-4} or $10^{-5} cm^2/V$ (66). The range estimate may be in error as it is likely to be sensitive to the Fe^{2+} impurity. The activation energy E_a for the loss of this Ag^{+} ion from the Fe^{2+} hole complex can be estimated from:

$$\nu = \nu_o \exp(-E_a/kT) \qquad 8.1$$

where ν_o is an ionic vibrational frequency assumed as $10^{13} sec^{-1}$. Equation 8.1 gives $E_a = 0.22 \pm 0.02$eV. Since the activation energy for diffision of Ag^{+} ions interstitially through the lattice is 0.10eV, the ion is free to diffuse away through the crystal once it has left the site near the iron.

Data is not available for the electron lifetime in AgBr, and hence the same estimate cannot be made. In any case the lowest temperature at which the Fe^{2+} ion may stably trap a hole is not known as no trigonal complex corresponding to the loss of a single Ag^{+} ion was detected.

Experiments aimed at investigating the properties of $3d^3$ ions in silver chloride have not been successful. Vanadium probably entered the lattice at least partly as V^{2+} but spectra were insufficiently well resolved to be analysed. Manganese is evidently stable as the divalent ion, spectra being detected over a year after crystal growth with little loss of intensity. No treatment altered the spectrum and thus if the tetravalent $3d^3$ ion is formed it is only in comparatively small concentrations. Chromium is known to be stable in the divalent form in silver chloride (67), and in view of the above lack of success, experiments planned to see whether the monovalent $3d^5$ or trivalent $3d^3$ ions could be stabilized were abandoned. Although hole centres must be formed in both AgCl and AgBr if only transiently, no E.S.R. has been detected which may be due to such a centre.

8.2 Calcium Oxide

In contrast to the silver halides, crystals of the alkaline earth oxides show E.S.R. spectra due to many impurities in the nominally undoped state. No purgative process such as zone refining is possible at present, and thus investigation must proceed on the assumption that there are significant concentrations of many impurities present.

Treatment in various atmospheres of vapour at elevated temperatures, when at least vacancy diffusion can occur, results in many changes of valence amongst the impurities, and the introduction of intrinsic defects. In the case of calcium oxide for example, impurities such as Mg^{2+} and Al^{3+} which are chemically similar to the host cations are resistant to valence changes, and thus most of the changes occur to the transition metal impurities. Generally smaller concentrations of anion impurities are present.

(a) Ionizing radiation

While ionizing radiation cannot change the overall state of the crystal, the evidence is very strong that redistribution of electrons may take place amongst the transition metal impurities and the intrinsic defects. This results in an increase of the valency of some defects and a decrease in the valency of others. It is assumed that charge neutrality over the crystal remains. The proportion of a particular ion that may change valency in these conditions depends on the state of the crystal before irradiation. For example in non stochiometric reduced crystals no spectra are detected for Fe^{3+}. After ultra violet irradiation it may be weakly detected. If the same crystal is oxidized an enhanced Fe^{3+} spectrum is observed, which may be further increased by ultra violet irradiation.

It has been shown that the growth process can in some circumstances produce non stochiometrically reduced crystals. These contain F and F^{+} centres in low concentrations, and the exceptionally small

linewidth has enabled the hyperfine parameters from the naturally occurring concentration of the Ca^{43} isotope, only 0.13% abundant, to be measured. These are A = 9.17 gauss, B = 0.97 gauss. Further spectra with splittings an order of magnitude smaller have been tentatively assigned to interaction with O^{17} nuclei, only 0.037% abundant. These parameters are A = -0.87 gauss, B = 0.05 gauss. The spectra were obtained at room temperature to avoid saturation problems, under continuous ultraviolet radiation, which by ionizing F centres, enhanced the F^+ spectrum. The reduced crystals contained many transition metal impurities in low states of valence, and a transiently stable spectrum was observed at room temperature which has been assigned to the $3d^3$ ion Ti^+ in an octahedral environment from its isotropic g value and nuclear splittings. This spectrum was also formed by irradiating at $77^{\circ}K$, but in this case the stability of the centre, even at room temperature was much greater. It is assumed that the Ti^+ ion is formed by a Ti^{2+} ion trapping an electron. The temperature dependence of the production of the spectrum suggests that the electron donors may be different in the different temperature ranges. The E.S.R. parameters of the spectrum are g = 1.9925 and $A^{47} = A^{49} = 11.7$ gauss.

(b) Oxidizing treatment - enhanced effects by ultra violet irradiation

Small concentrations of V_1 centres could also be produced in these reduced crystals by ultra violet irradiation, but oxidation generally increased the concentration. Further ultra-violet irradiation gave rise to a considerable further enhancement of the spectrum.

The observation of some hole centres which were stable at room temperature in contrast to other workers' results is suggested to be a consequence of the rather low impurity content in these crystals compared with other calcium oxide crystals. The decay of V centres at room temperature must be associated with the trapping of electrons which have been thermally ionized from nearby defects. A proportion of the V centres is assumed to be sufficiently far from such other defects, so as to have negligible trapping probability. The parameters of the V centres are listed in Table 7.5.

The low overall concentration of paramagnetic defects that may contribute to spin spin broadening and the small amount of strain, has enabled resolution of the hyperfine parameters of Gd^{3+} for the first time. They have been found to be A^{155} = 3.9 gauss and A^{157} = 5.1 gauss.

A spectrum observed after rapid quenching has been attributed to double quantum transitions in the Mn^{2+} spectrum. A necessary assumption has been the addition of a D term to the Hamiltonian for the ion, which will arise from axial distortions of the symmetry. This is not surprising as distortion of the crystal field will inevitably result from such rapid cooling of the crystal. It is not clear how this spectrum is produced or enhanced by ultra-violet irradiation. If it is assumed that the only effect of the radiation is to produce valence changes, then it is difficult to see how sufficient Mn^{2+} ions undergo axial distortion of the crystal field without interacting with paramagnetic centres resulting from the valence change. Previous workers

observing double quantum transitions in magnesium oxide have not specified the treatment the crystals underwent before observation of such spectra.

8.3 Suggestions for Future Work

A number of possible lines for future work are evident from this thesis. Most obviously the long lived fluorescence needs explanation since no resonance could ultimately be attributed to a triplet state of the F centre. A computation of the g value of ^3P level gave g = 1.5 (68) but a search in this region failed to reveal any spectra. Apparently the resonance is unlikely to be observed because of the Jahn Teller effect (68). The transiently stable Ti^+ spectrum may be formed via an excited state, or an excited state may be populated from the ground state following formation of Ti^+ from Ti^{2+}. At 77°K the E.S.R. spectrum was less intense under irradiation and this is most probably due to population of an excited state. The return of full intensity after irradiation had about the same time constant as the decay of the fluorescence. While emission has been observed from $3d^3$ ions in magnesium oxide (1), this occurred from the ^2E to ground state and is an allowed transition which would not have a long lifetime.

Complex spectra in neutron irradiated calcium oxide which may be due to aggregated F centre spectra have not been analysed. Such spectra have been observed in magnesium oxide (1). Further spectra associated with the F^+ spectrum in reduced calcium oxide have not been

analysed either. The spectra are inefficiently enhanced by ultra violet radiation at room temperature. Irradiation at lower temperatures may prove more useful for enhancing them. The total splittings of the neutron induced centres are about 100 gauss and the ultra violet induced centres about 10 gauss.

The changes in most of the E.S.R. spectra during ultra violet irradiation have been explained in terms of a redistribution of the available electrons among the defects. Two anomalies stand out which do not seem to be explained by the above idea. First, during irradiation of any of the samples at 77^{o}K, the largest proportion of defects trapped holes to become more positively charged. The ions Fe^{3+} and Cr^{3+} were formed in large intensities, and there was no sign of reduction except in the case of Ti^{+} which had a fairly low integrated intensity. A possible explanation would be that the Fe^{2+} as well as going to Fe^{3+} was going to Fe^{1+}, but this ion was not detected at the temperatures used. Secondly the increase in V centres of all types with irradiation and the increased intensity of the double quantum transitions of Mn^{2+} could most obviously be explained in terms of vacancy diffusion from the surface. In the alkali halides where low energy ionizing radiation has been successful in producing ionic displacements, a simple mechanism of exciton decay by non-radiative transitions may in suitable cases dissipate the exciton energy in a replacement collision sequence along a line of anions. Similar calculations for a replacement collision in the 110

direction in magnesium oxide give threshold energies of 40eV (69). While it may be expected that the equivalent process would require less energy in calcium oxide, it seems unlikely that radiation with very few photons above 4.9eV would create vacancies (even cation vacancies which may require less energy) in appreciable numbers.

REFERENCES

1. B. Henderson and J.E. Wertz, to be published.
2. A.H. Kahn and C. Kittel, Phys. Rev. 89 315 (1953)
3. A.F. Kip, C. Kittel, R.A. Levy and A.M. Portis, Phys. Rev. 91 1066 (1953).
4. G. Feher, Phys. Rev. 105 1122 (1957).
5. J.E. Wertz, P. Auzins, R.A. Weeks and R.H. Silsbee, Phys. Rev. 107 1535 (1957).
6. J.C. Kemp, W.M. Ziniker and J.A. Glaze, Proc. Brit. Cer. Soc. 9 109 (1967).
7. A.J. Tench and R.L. Nelson, Proc. Phys. Soc. 92 1055 (1967).
8. J.C. Kemp, W.M. Ziniker and E.B. Hensley, Phys. Letters 25A 43 (1967).
9. J.E. Wertz, J.W. Orton and P. Auzins, J. Appl. Phys. 33 suppl. 322 (1962).
10. J.E. Wertz, P. Auzins, J.H.E. Griffiths and J.W. Orton, Disc. Far. Soc. 28 136 (1959).
11. W. Low and E.L. Offenbacher, Sol. State Phys. 17 135 (1965).
12. J.S. van Wieringen and J.G. Rensen, Proc. 1st Int. Conf. Paramagnetic Res. 1 105 (1962).
13. D.J.E. Ingram, 'Spectroscopy at Radio and Microwave Frequencies' 2nd Ed. (Butterworths, 1967).
14. W. Hayes, J.R. Pilbrow and L.M. Slifkin, J. Phys. Chem. Solids 25 1417 (1964).
15. W. Low, Phys. Rev. 105 801 (1957).
16. F.A. Cotton, 'Chemical Applications of Group Theory' (Wiley, 1964).

17. A. Abragam and H.M.L. Pryce, Proc. Roy. Soc. A205 135 (1951).

18. A. Carrington and A.D. McLachlan, 'Introduction to Magnetic Resonance' (Harper, 1967).

19. A.M. Stoneham, A.E.R.E. Report R5530 (1967).

20. J.E. Wertz, J.W. Orton and P. Auzins, Disc. Far. Soc. 31 140 (1961).

21. C.P. Poole Jr., 'Electron Spin Resonance' (Interscience, 1967).

22. P.V. McD. Clark and J.W. Mitchell, J. Photo. Sci. 4 1 (1956).

23. W. Pfann, 'Zone Melting' (Wiley, 1958).

24. H.D. Koswig and I. Kunze, Phys. Stat. Sol. 8 319 (1965).

25. D.H. Lindley and P.G. Debrunner, Phys. Rev. 146 199 (1966).

26. A.N. Murin et al., Sov. Phys. Sol. State 8 2632 (1967); ibid. 9 1110 (1967).

27. K. Hennig, Phys. Stat. Sol. 3 91 (1963).

28. K.A. Hay, Ph.D. Thesis, Keele University, U.K. (1966).

29. K.A. Hay, New York A.P.S. Meeting (1967).

30. K.A. Hay, D.J.E. Ingram and A.C. Tomlinson, to be published.

31. M.U. Palma, to be published.

32. J.W. Mitchell, Rept. Prog. Phys. 20 443 (1957).

33. J. Schneider and S.R. Sircar, Zeitschrift fur Naturforschung 17A 155 (1962).

34. B. Henderson and T.P.P. Hall, Proc. Phys. Soc. 90 511 (1967).

35. G. Kuwabara, Phys. Rev. 138 A99 (1965).

36. R.F. Tucker Jr., Phys. Rev. 112 725 (1958).

37. V.I. Neeley and J.C. Kemp, Bull. Am. Phys. Soc. 8 484 (1963).

38. R.W. Soshea, A.J. Dekker and J.P. Sturtz, J. Phys. Chem. Sol. 5 22 (1958).

39. W. Low and R.S. Rubins, Proc. 1st Int. Conf. Paramagnetic Res. 1 79 (1962).

40. A.J. Shuskus, Phys. Rev. 127 2022 (1962).

41. J.M. Baker, B. Bleaney and W. Hayes, Proc. Roy. Soc. A247 141 (1958).

42. W. Low, Paramagnetic Resonance in Solids, suppl. to Vol. 2, Solid State Physics (1960).

43. D.R. Speck, Phys. Rev. 101 1725 (1956).

44. A. Bohr and V.F. Weisskopf, Phys. Rev. 77 94 (1950).

45. W. Low and D. Shaltiel, J. Phys. Chem. Sol. 6 315 (1958); Phys. Rev. 115 424 (1959).

46. C.F. Hampstead and K.D. Bowers, Phys. Rev. 118 131 (1960).

47. J.E. Wertz, G.S. Saville, L. Hall and P. Auzins, Proc. Brit. Cer. Soc. 1 59 (1964).

48. H.M. Zaripov, V.S. Kropotov, L.D. Livanova and V.G. Staponov, Sov. Phys. Sol. State 9 992 (1967).

49. J. Owen and J.H.M. Thornley, Reports on Progress in Physics 29 675 (1966).

50. H. Seidel, Lecture to NATO summer course on Paramagnetic Defects in Crystals (1967).

51. J.E. Wertz, J.W. Orton and P. Auzins, Disc. Far. Soc. 31 140 (1961).

52. B. Henderson, Paper presented to Int. Conf. on Mass Transport in Oxides, Washington U.S.A. (1967).

53. H. Kon and N.E. Sharpless, J. Phys. Chem. 70 105 (1966).

54. K. De Armond, B.B. Garrett and H.S. Gutowsky, J. Chem. Phys. 42 1019 (1965).

55. W. Low and J.T. Suss, Int. Conf. on Electron Diffraction and Crystal Defects II B-1 Melbourne (1965).

56. A.J. Shuskus, J. Chem. Phys., 39 849 (1963).

57. F. Seitz, Rev. Mod. Phys., 26 7 (1954).

58. R. Wyckoff, 'Crystal Structures' Vol. I, 2nd Ed. (Interscience 1963).

59. P.W. Kirklin, P. Auzins and J.E. Wertz, J. Phys. Chem. Sol. 26 1067 (1965).

60. A.J. Shuskus, Phys. Rev. 127 1529 (1962).

61. W. Low, Phys. Rev. 105 793 (1957).

62. J.W. Orton, P. Auzins and J.E. Wertz, Phys. Rev. Letters, 4 128 (1960).

63. P.V. Auzins and J.E. Wertz, J. Phys. Chem. 71 211 (1967).

64. E.R. Feher, Phys. Rev. 136 A145 (1964).

65. K. Kobayashi and F.C. Brown, Phys. Rev. 113 508 (1959).

66. R.S. Van Heyningen and F.C. Brown, Phys. Rev. 111 462 (1958).

67. H.D. Koswig and I. Kunze, Phys. Stat. Sol. 9 451 (1965).

68. R.H. Bartram, unpublished.

69. D. Pooley, Proc. Phys. Soc. 87 245 and 257 (1966).

70. W.C. Holton and H. Blum, Phys. Rev. 125 89 (1962).